

LOAN ONLY

# The Institute of Paper Chemistry

Appleton, Wisconsin

## Doctor's Dissertation

A Study of Particle Retention in Relation  
to the Structure of a Fibrous Mat

Robert C. Johnson

June, 1962

**LOAN COPY**  
To be returned to  
**EDITORIAL DEPARTMENT**

A STUDY OF PARTICLE RETENTION IN RELATION  
TO THE STRUCTURE OF A FIBROUS MAT

A thesis submitted by

Robert C. Johnson

B.S. 1956, Michigan College of Mining and Technology  
M.S. 1958, Lawrence College

in partial fulfillment of the requirements  
of The Institute of Paper Chemistry  
for the degree of Doctor of Philosophy  
from Lawrence College,  
Appleton, Wisconsin

June, 1962

## TABLE OF CONTENTS

	Page
INTRODUCTION	1
ANALYSIS OF THE PROBLEM	4
Requirements of a Theoretical Approach to the Problem of Retention of Particles by the Internal Structure of a Filter Medium	4
An Alternative Approach	5
Actual System Used	5
Possible Mechanisms by Which a Particle May be Removed from a Fluid by a Cylindrical Fiber	6
Models of a Fibrous Mat	6
Collection Mechanisms	7
Parameters Relating the Collection Efficiency of a Cylinder to the System Variables	15
The Effective Fiber Efficiency	15
The Inertial Impaction Parameter	15
The Flow Line Interception Parameter	17
The Diffusion Parameter	18
The Settling Parameter	19
Other Approaches	19
Experimental Investigations of the Removal of Fine Particles by the Internal Structure of Filter Materials	20
Summary and Experimental Approach	23
EXPERIMENTAL	25
Apparatus	25
Materials	31
Fibers	31
Particles	33

	Page
Water	38
Procedures	41
Mat Formation	41
Filtration Experiment	42
Analysis	43
Results and Discussion	45
Effective Fiber Efficiency of a Cylindrical Fiber in a Mat of Fibers	45
Assumptions in Derivation	47
Presentation and Analysis of Data	56
Determination of the Effective Fiber Efficiency	56
Effect of Fluid Velocity and Fiber Diameter on $\eta$	56
Effect of Mat Porosity on $\eta$	59
Probable Controlling Mechanism of Collection	63
Confirmation of Brownian Diffusion as Controlling Mechanism of Retention	65
Final Correlation of Data	66
Physical Significance of the Correlation	70
Comparison of Data with Theoretical Results	72
SUMMARY AND CONCLUSIONS	75
Approach Used	75
Results	75
Conclusions	77
Future Work	78
NOMENCLATURE	82
ACKNOWLEDGMENTS	84
LITERATURE CITED	85

	Page
APPENDIX I. EFFECT OF IONIC CONDITIONS ON RETENTION	87
Formation of a Stable Titanium Dioxide Suspension	87
Experiments Leading to the Selection of the Present Suspension Media	87
APPENDIX II	92

## INTRODUCTION

Many chemical process industries require the removal of solid particles from a fluid stream at one or more phases in their operation. This separation is usually accomplished by filtration, either alone, or combined with settling or centrifugation.

Industrial filtrations can be classified into two types: "cake filtration," and "media filtration."

In cake filtration, the particles do not pass through the openings in the media, but are retained on the surface. As more and more particles are retained, a "cake," or layer of particles forms on the surface of the filter media. Additional particles are deposited on the surface of this "cake," and the fluid passes around and between the particles making up the "cake."

Cake filtration is usually used where particles are large, or can easily be agglomerated into large aggregates. Two examples of cake filtration in the pulp and paper industry are:

1. The washing or thickening of pulp;
2. The dewatering of calcium carbonate in the kraft recovery process.

Cake filtration is usually not used when the suspension to be filtered contains a small amount of small, well-dispersed particles that cannot be agglomerated. In this case, the particles form a cake with a low void fraction and a very high resistance to flow. "Media filtration" is usually used in this case, the particles being retained by the internal structure of a thick, high porosity filter media. The

increase in the resistance of the filter mat due to the deposition of the particles is small compared to the increase that would have occurred if the particles had been deposited in a cake on the surface of the filter media.

"Media filtration" is used extensively in air filtration; and where the fluid is a liquid, it is called "solution clarification." A few examples of industrial filtrations where the particles are retained by the internal structure of the filter media are:

1. The clarification of municipal water supplies by passing them through thick beds of sand or diatomaceous earth.
2. The "blinding" of filter media used in cake filtration. Occasional fine particles are not removed at the surface of the media, but are retained by the internal structure. Eventually, these small particles completely fill the void spaces in the media, increasing the resistance of the media to flow tremendously.
3. Media filtration is also important in the retention of fine inorganic filler materials in commercial sheet-making operations.

While cake filtration is fairly well understood, the retention of particles by the internal structure of a filter media is a much more complex phenomenon, and is very poorly understood. Very little work has been done to determine the mechanisms which cause the particles in the fluid to move from the fluid to the internal surface of the filter media.

Also, very little is known about the attractive forces causing the particles to adhere to the internal surfaces, or their order of magnitude compared to the fluid drag forces and repulsive forces.



## ANALYSIS OF THE PROBLEM

### REQUIREMENTS OF A THEORETICAL APPROACH TO THE PROBLEM OF RETENTION OF PARTICLES BY THE INTERNAL STRUCTURE OF A FILTER MEDIUM

A rigorous theoretical approach to a study of solution clarification would be very desirable at this time. This would require a description of the geometry and spatial arrangement of the structural elements of the filter media, and a knowledge of the equations of motion of the fluid around these elements. Next, a description of the motion of the particles with respect to the fluid would be required. This would take into account Brownian motion of the particles, the effect of gravity on the particles, the motion of the particles caused by Van der Waal's attractive forces, and the electrostatic attractive or repulsive forces due to charges on the surfaces of the particles or structural elements of the filter. The inertial properties of the particles would also be important, as the velocity vectors of the particle and the fluid will not necessarily be the same in regions where the fluid velocity vector is changing direction and/or order of magnitude rapidly.

If all the properties of the particles, fluid, and filter media mentioned above could be described mathematically, solution of the equations of motion of the particles and the fluid to obtain the probability of collision between a particle and the structural elements of the filter media would be difficult, if not impossible, for the general case.

A few attempts have been made to determine the probability of collision between a spherical particle and a single cylinder in an infinite fluid stream under idealized conditions. These will be discussed later.

#### AN ALTERNATIVE APPROACH

In investigations of a complex phenomenon, such as solution clarification, where a rigorous theoretical approach is not possible, a systematic, stepwise approach is the best alternative.

If a well-defined system is used, it should be possible to analyze the system to determine the important variables and the possible mechanisms of retention. The variables can then be investigated, one at a time, to determine which variables actually influence retention, and the order of magnitude of their influence. The results can then be analyzed to determine the controlling mechanisms of retention over the range of variables investigated. This was the approach used in this study.

#### ACTUAL SYSTEM USED

The paper industry is very interested in the retention of inorganic filler materials in the formation of a sheet of paper. They are concerned not only with the total amount retained, but also the location of the material in the final sheet.

The formation of a sheet of paper on a paper machine is an extremely complex process of filtration of the suspension of fibers, forming a

filter mat of constantly changing properties, in which the filler materials are then retained. In this process, not even the retention of the fibers on the wire is completely understood. The filter mat which is being formed is composed of fibers of widely varying size, shape, and orientation. Further, the filter mat has a nonuniform porosity, resulting in a nonuniform fluid velocity in the mat. Also, the velocity may vary from point to point in one plane in the sheet because the sheet was formed from a flocculated suspension.

Although the retention of fine particles of filler materials by the internal structure of a sheet of paper during its forming process is of immediate interest, the papermaking system is obviously too complex a system to use for initial investigations of the phenomenon of solution clarification. Therefore, for this investigation the following simplified system was used. The retention studies were made using a preformed mat, which had been compacted to a uniform porosity with a permeable piston. The filter mat was made up of solid cylindrical fibers having a narrow diameter range. The mat was formed by filtration of a dilute, unflocculated suspension of the fibers. This produced a structure with the fibers randomly oriented in the X-Y plane, almost completely perpendicular to the direction of flow (in the Z direction).

#### POSSIBLE MECHANISMS BY WHICH A PARTICLE MAY BE REMOVED FROM A FLUID BY A CYLINDRICAL FIBER

#### MODELS OF A FIBROUS MAT

A number of models have been used to describe flow through porous media. These have been reviewed by Scheidegger (1), and only two models commonly used with fibrous porous media will be mentioned here.

The hydraulic radius theory pictures the fibrous mat to be a network of tortuous capillaries having irregular cross sections. The Kozeny-Carman version of the hydraulic radius theory has been used very successfully to describe the flow rate-pressure drop relationship in a fibrous mat (2, 3). Hermans and Bredée (4) and Grace (5) used this type of a model to explain the retention of particles by the internal structure of a fibrous filter media. They hypothesized that the particles were collected on the walls of the capillary, reducing its radius and increasing its resistance to flow.

The fiber drag theory pictures the fibrous mat as layers of cylindrical fibers perpendicular to the direction of flow, and assumes that the flow pattern around these fibers is the same as around a single cylindrical fiber in an infinite fluid medium. This is not quite the case; at low Reynolds numbers the cylinder influences the flow pattern many diameters upstream and downstream. Therefore, adjacent fibers in the Z direction will disturb the flow pattern around each other. While no one has successfully applied the fiber drag theory to describe the flow rate-pressure drop relationship in a fibrous mat, application of this model allows the prediction of some of the mechanisms of collection of particles from a fluid by the fibers in a mat. Some of the predicted mechanisms have been experimentally verified in studies of air filtration, as will be shown later.

#### COLLECTION MECHANISMS

Eight mechanisms by which aerosols\* can be deposited on surfaces have been demonstrated:

---

\*The word "aerosol" used here means a suspension of small solid or liquid particles in a gas.

1. Inertial impaction
2. Flow line interception
3. Brownian diffusion
4. Settling
5. Electrostatic attraction
6. Sieving or plugging
7. Eddy diffusion
8. Thermal deposition

1. When a fluid flows past a cylinder, the streamlines begin to curve around the cylinder an appreciable distance upstream. If a particle in the fluid has the same density as the fluid, it will follow the fluid streamlines. If the particle has a density greater than the fluid density, its inertia will resist the acceleration of the fluid in the X direction (Fig. 1), and it will move across the streamlines toward the cylinder, increasing the probability of collision with the cylinder. The movement of the particle is resisted by viscous forces according to Stokes' law.

2. If a particle has the same density as the fluid, but has a finite size, it will collide with the cylinder if the streamline containing the center of the particle passes less than one-half the diameter of the particle away from the surface of the cylinder (Fig. 2). Note that this is also a boundary condition for all other mechanisms of collection; collision will occur when the center of the particle is a distance  $\frac{D_p}{2}$  from the fiber.

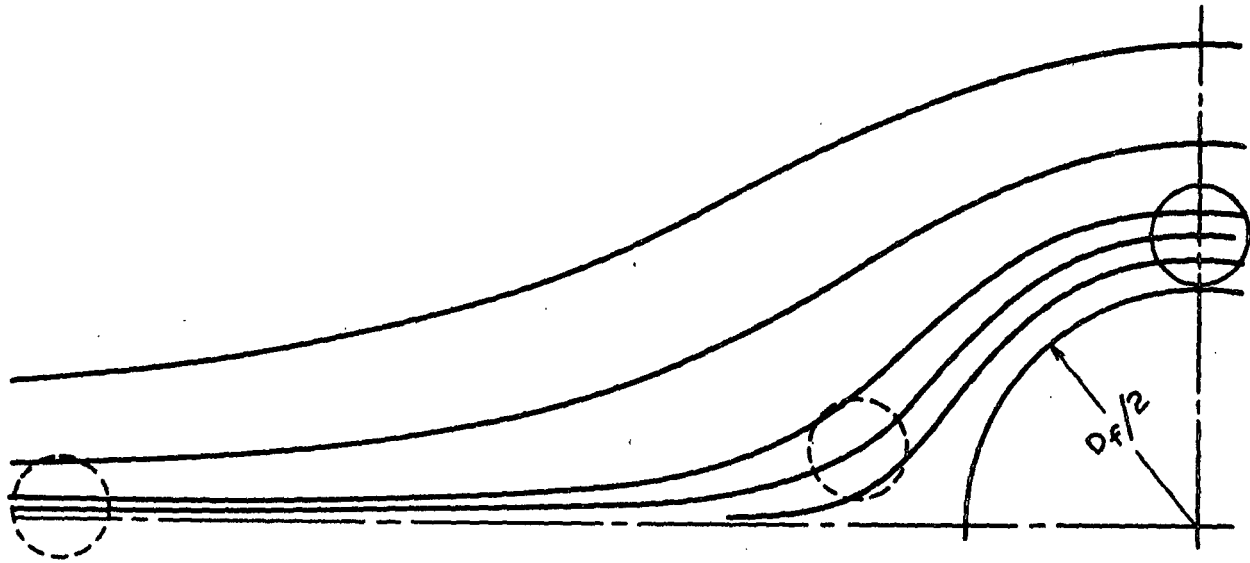


Figure 2. Pictorial Representation of the Flow Line Interception Mechanism of Collection

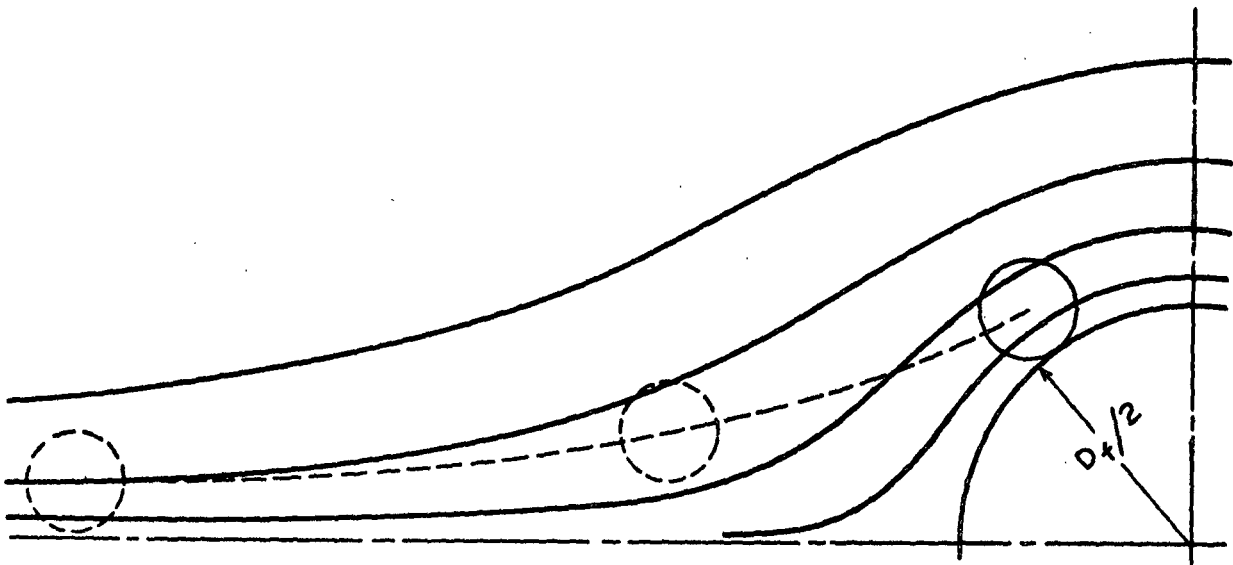


Figure 1. Pictorial Representation of the Inertial Impaction Mechanism of Collection

3. Small particles suspended in a fluid exhibit Brownian movement because of collisions with the fluid molecules. This random movement may result in a particle, whose center was originally in a streamline which would not pass close enough to the cylinder for a collision to occur, moving across the streamlines and colliding with the cylinder (Fig. 3).

4. Any particle having a density greater than the fluid density will have a finite velocity relative to the fluid in the minus Z direction, due to the force of gravity. As the fluid streamlines curve around the cylinder, this component of the particle velocity will cause the particle to move across the streamlines toward the fiber, increasing the probability of collision. (If the flow is in the plus Z direction, the probability of collision will be decreased by this mechanism.) (See Fig. 4.)

5. Electrostatic attraction is an important collection mechanism in aerosol filtration (6). If both the fiber mat and the particles are charged, a coulombic force will greatly increase, or decrease (depending on the signs of the two charges), the probability of collision of the particle and a fiber in the mat. If only the particles or the fibers are charged, there will still be an electrostatic attraction due to induction of an opposite charge in the uncharged members.

In a system containing a conducting liquid, one would expect immediate grounding of these charges, and this undoubtedly is what happens to friction-generated charges. However, another charging

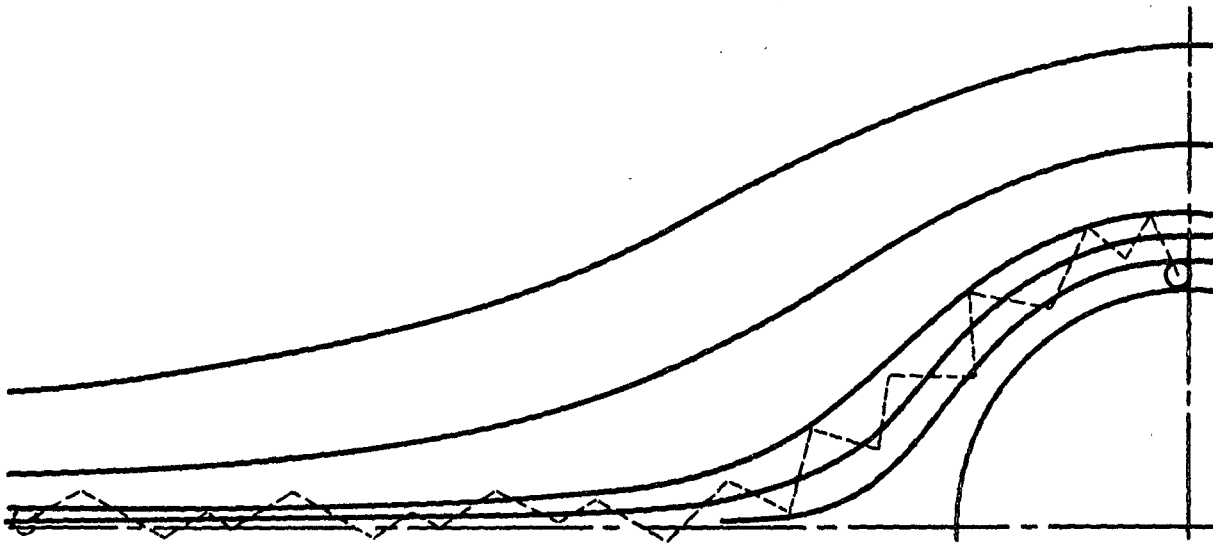


Figure 3. Pictorial Representation of the Diffusion Mechanism of Collection

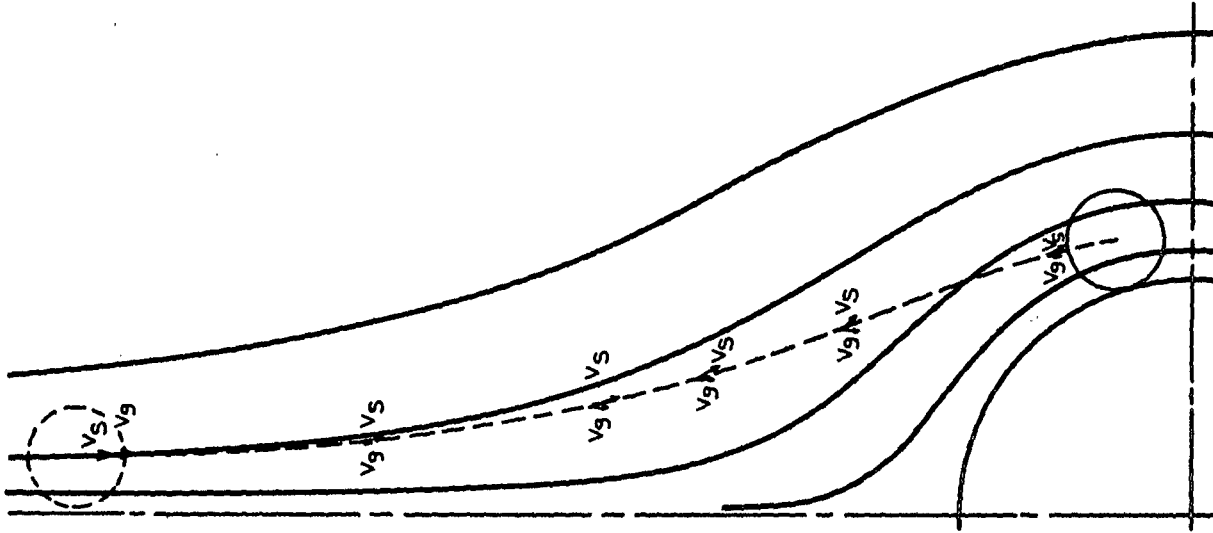


Figure 4. Pictorial Representation of the Settling Mechanism of Collection  
 $V_s$  is the Velocity of the Fluid Streamline,  
 $V_g$  is the Stokes' law Settling Velocity of the Particle



mechanism exists. In a liquid containing ions, preferential adsorption of the ions takes place at the solid-liquid interface, producing a diffuse double layer of ions and a potential difference between the interface and the bulk liquid (see Fig. 5). A portion of the ions are tightly bound to the surface and cannot be removed by movement of the liquid. The remainder of the diffuse double layer can be removed by movement of the liquid, and, therefore, some of the potential difference is also mobile. The mobile part of the potential drop, the potential drop between the bound layer and the bulk liquid, is called the zeta potential. It is responsible for the repulsive force between adjacent particles when they are close enough so their diffuse double layers overlap. Holtzman (7) has shown by use of the Verwey and Overbeek theory that, by increasing the ionic concentration of the particle suspension, the thickness of the electrical double layer can be reduced to the point where the distance over which the repulsive forces due to adsorbed ions act is such that the Van der Waal's forces of attraction are always greater than the repulsive forces. Thus, it appears that, if the proper ionic concentration is maintained, the electrical effects due to adsorbed ions should not influence the probability of collision of a particle and a cylinder. However, the electrical effects might affect the initial adhesion of the particle and the cylinder.

6. Some collection of particles by the internal structure of a fiber mat probably takes place by sieving, or plugging of a flow channel which is smaller than the particle. If one assumes that the number of fibers in the previously described mat that are parallel and

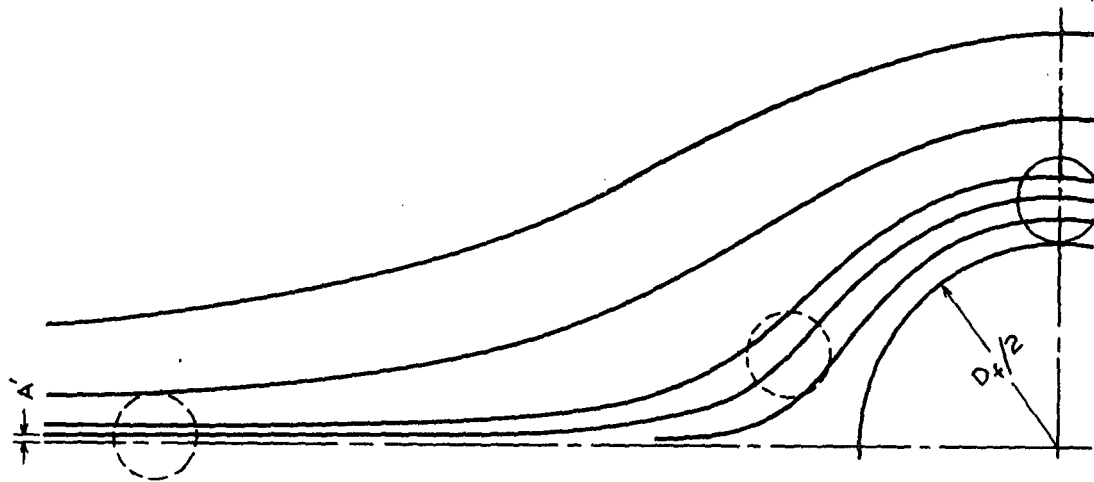


Figure 6. Pictorial Representation of the Definition of Collection Efficiency for a Case Where the Flow Line Interception Mechanism of Collection is Controlling

$$\eta_0 = 2A'/D_+^2$$

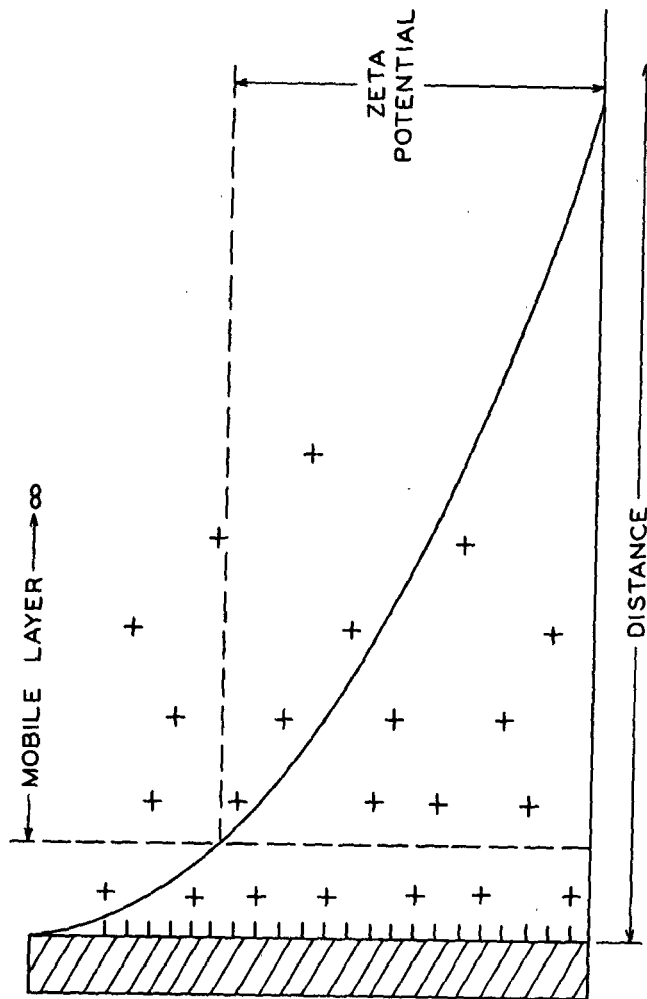


Figure 5. Partial Representation of the Diffuse Double Layer of Ions Adsorbed by a Particle and the Potential Produced

less than one fiber diameter apart is negligible, then the smallest flow channels between fibers will occur at intersections of three fibers. A little manipulation with three pieces of rubber tubing will show that the smallest opening that can be made between the three "fibers" is large enough to pass a particle with a diameter about one-fourth the diameter of the "fibers." Very little flow will take place through such a small opening and the number of these intersections occurring in a fiber mat is probably small. If the particle-diameter-to-fiber-diameter ratio used is less than one half, the amount of particles retained by a fiber mat by a sieving action should be very small compared to the total amount retained.

7. Friedlander (8) has studied the deposition of aerosols from turbulent gas streams where the controlling mechanism was eddy diffusion. This investigation will be carried out in a region where the flow is streamline rather than turbulent. At Reynolds numbers based on the fiber of about one, there is some eddy formation on the downstream side of the fiber, but particle deposition by eddy diffusion is expected to be negligible.

8. It has been shown that small particles in a temperature gradient are subjected to a force which causes them to move toward the colder surface (9). These thermal forces are small and proportional to the temperature gradient. Since the fiber mat and fluid stream are at essentially the same temperature in a liquid filtration, this mechanism is not important in liquid filtration.

It appears that only four mechanisms of collection will be operating in solution clarification in the streamline flow region: 1. inertial impaction; 2. flow line interception; 3. Brownian diffusion; and 4. settling. All four mechanisms will act to increase the collection of particles by the fiber mat; but over various ranges of fluid velocity, fiber size, particle size, and particle density, one of the mechanisms may have a far greater effect than the others, and be controlling.

#### PARAMETERS RELATING THE COLLECTION EFFICIENCY OF A CYLINDER TO THE SYSTEM VARIABLES

##### The Effective Fiber Efficiency

In the remainder of this work, the probability of collision of a particle with a fiber and the collection of particles by a single fiber, or a fiber in a mat, will be discussed in terms of the effective fiber efficiency. The symbol,  $\eta_o$ , will be used for the effective fiber efficiency of a single cylinder in an infinite fluid medium, and  $\eta$  will be used for the effective fiber efficiency of a cylindrical fiber in a mat of fibers.

The effective fiber efficiency,  $\eta_o$ , is defined as the ratio of the number of particles collected by the fiber per unit time to the number of particles in the fluid stream passing through an area equal to the projected area of the fiber per unit time. This is illustrated for a case with the flow line interception mechanism controlling in Fig. 6. ✓

##### The Inertial Impaction Parameter

The inertial impaction parameter,  $\psi$ , is equal to:

$$\psi = \frac{(\rho_p - \rho_f) v_o D_p^2}{18 \mu D_f} \quad (1)$$

where:

$\rho_p$  = the density of the particle, g./cc.

$\rho_l$  = the density of the liquid, g./cc.

$V_o$  = the velocity of the fluid stream approaching the cylinder, cm./sec.

$D_p$  = the diameter of the particle, cm.

$\mu$  = the fluid viscosity, poises

$D_f$  = the diameter of the collecting cylinder or fiber, cm.

Wong (10) has discussed the physical significance of the inertial impaction parameter.  $\psi$  represents the ratio of the stopping distance in a still fluid of a spherical particle having an initial velocity  $V_o$ , and moving according to Stokes' law, to the diameter of the cylinder.  $\psi$  also represents the ratio of the force necessary to stop a particle initially travelling at a velocity  $V_o$  in a distance  $D_f/2$  to the Stokes' law fluid resistance on a particle moving with a relative velocity  $V_o$ .

What is of more theoretical significance, however, is the fact that  $\psi$  appears as a multiplying factor when the equations of motion for a particle relative to a fluid stream flowing around a cylinder are put into dimensionless form (in the absence of an external force field, and where Brownian motion is negligible).

Theoretically, it should be possible to solve these equations for a given velocity field around a cylinder to get the collection efficiency. However, the velocity field is a function of the Reynolds number,  $Re$ , and the limiting trajectory of a particle which is collected does not have to touch the cylinder, but just approach within  $D_p/2$  of it. Thus, the

collection efficiency by inertial impaction is a complex function of  $\psi$ ,  $\underline{Re}$ , and  $\underline{D_p}/\underline{D_f}$ . Wong (10) has reviewed the numerical calculations of  $\eta_o$  versus  $\psi$  for several velocity fields that are in the literature. He has also shown experimentally that the collection efficiency of an isolated cylindrical wire, in a region where direct interception is very small, is a strong function of  $\psi$ , and increases slightly with increasing values of  $\underline{Re}$  and  $\underline{D_p}/\underline{D_f}$ . The experimental values of  $\eta_o$  agreed with the predicted values reasonably well.

#### The Flow Line Interception Parameter

The flow line interception parameter has been defined as  $\underline{D_p}/\underline{D_f} = \underline{R}$ . The collection efficiency of a cylinder for the flow line interception mechanism is not a simple function of  $\underline{R}$ , however. The area of the original fluid stream from which the particles are collected is a function of the fiber diameter and of the flow pattern around the cylinder, which is a function of the Reynolds number,  $\underline{Re}$ .

Langmuir (11) has used Lamb's equation (12) for the velocity distribution around an isolated cylinder to derive an equation for the collection efficiency as a function of  $\underline{R}$  and  $\underline{Re}$ . He obtained:

$$\eta_o = \frac{1}{2(2.002 - \ln \underline{Re})} \left[ 2(1 + \underline{R})\ln(1 + \underline{R}) - \frac{\underline{R}(2 + \underline{R})}{(1 + \underline{R})} \right] \quad (2)$$

The use of Lamb's equation limits the use of Equation (2) to Reynolds numbers (based on the cylinder) of less than two, small values of  $\underline{R}$  (probably less than 0.2), and assumes that the particle does not alter the velocity distribution around the fiber as it approaches the fiber

or after it adheres to the fiber. It also assumes adhesion of the particle to the fiber once collision takes place.

### The Diffusion Parameter

Einstein (22) has shown that the diffusion coefficient of an aerosol particle should be:

$$D_{BM} = kT/3\pi \mu D_p \quad (3)$$

where:

$D_{BM}$  = diffusion coefficient, sq. cm./sec.

$k$  = Boltzmann's constant,  $1.380 \times 10^{-16}$  erg./deg.

$T$  = absolute temperature, degrees Kelvin

Langmuir (11) has shown from the random walk theory that the average value of the displacement,  $\bar{x}$ , of a particle in time,  $t$ , in a certain direction is given by:

$$\bar{x} = \left( \frac{4}{\pi} D_{BM} t \right)^{1/2} \quad (4)$$

Using Lamb's equation for viscous flow around a cylinder to approximate the effective distance and time of movement, he found that the effective thickness of the fluid layer from which particles are removed by diffusion and direct interception,  $x_o$ , is given by:

$$\frac{x_o}{D_f} = \left[ \frac{0.14 D_{BM}}{D_f V_o \left\{ \frac{1}{2(2.002 - \ln Re)} \right\}} \right]^{1/3} \quad (5)$$

Substituting Equation (5) back into Lamb's equation for flow around a cylinder, he arrived at Equation (6), which has the same

form as Equation (2):

$$\eta_o = \frac{1}{2(2.002 - \ln Re)} \left[ 2\left(1 + \frac{2x_o}{D_f}\right) \ln \left(1 + \frac{2x_o}{D_f}\right) - \frac{\left(\frac{2x_o}{D_f}\right)\left(2 + \frac{2x_o}{D_f}\right)}{1 + \frac{2x_o}{D_f}} \right] \quad (6)$$

Ranz (13) has called the ratio,  $\frac{D_{BM}}{D_f V_o}$ , the diffusion parameter,  $\underline{D}$ , and described its physical meaning as the ratio of an "effective force" causing Brownian motion in the direction of the collector to the fluid resistance at a relative particle velocity of  $\underline{V_o}$ . It might be noted that  $\underline{D}$  is equal to  $1/(\underline{Re})(\underline{Sc})$ .

The Schmidt number is the ratio of the molecular momentum transfer to molecular mass transfer.

#### The Settling Parameter

Ranz (13) has characterized settling by the parameter:

$$G = (\rho_p - \rho_l) g D_p^2 / 18 \mu V_o \quad (7)$$

where  $\underline{g}$  = the acceleration due to gravity, 981 cm./sec.<sup>2</sup>. Physically, this parameter represents the ratio of the free settling velocity of the particle to stream velocity.

#### Other Approaches

Thomas (17) has applied dimensional analysis to the problem of the collection of particles from a fluid stream by a cylindrical fiber in a mat of fibers. His analysis showed that retention should be a function of the following parameters:  $\underline{R}$ ,  $\underline{Re}$ ,  $\underline{Sc}$ ,  $\psi$ ,  $\underline{G}$ , and the porosity,  $\epsilon$ .



Dorman (20) has considered air filtration to be a random process without regard to the physical structure of the filter media. He states that, if filtration is a random process, then:

$$N_h = N_o e^{-\gamma} \quad (8)$$

The exponent,  $\gamma$ , should then be related to the thickness of the mat, and the several additive parameters for collection by inertial impaction, diffusion, and flow line interception. Thus,

$$\gamma = B [(C V_o^2 + E/(V_o)^{2/3} + I) h] \quad (9)$$

where:

$B$  = a constant

$C$  = Dorman's inertial impaction parameter

$E$  = Dorman's diffusion parameter

$I$  = Dorman's interception parameter

$h$  = mat thickness, cm.

$N_o$  = number of particles per unit volume of fluid at the surface of the mat, cm.<sup>-3</sup>

$N_h$  = number of particles per unit volume of fluid at the mat thickness equal to  $h$ , cm.<sup>-3</sup>

#### EXPERIMENTAL INVESTIGATIONS OF THE REMOVAL OF FINE PARTICLES BY THE INTERNAL STRUCTURE OF FILTER MATERIALS

Hermans and Brédee (4) have studied the constant pressure filtration of viscose. For the portion of the filtrate volume-time curve in which the particles were being retained by the internal structure of

the filter media, they found that the rate of change of the filtration resistance was proportional to the instantaneous resistance raised to the  $3/2$  power. They called this the "standard blocking law."

Grace (5) also found that this relationship fit the filtrate volume-time data for a large part of the filtration cycle for dilute suspensions of carbonyl iron particles smaller than the pore size of the filter media. Grace used many different woven filter media and determined the pore size by mercury intrusion and from permeability data. In the region where the equations fit the data, there was no visible cake formation on the upstream surface of the filter media.

Grace (14) also has presented a graph which indicates that the retention of monodisperse uniform polystyrene particles 1.17 microns in diameter is very closely related to the average pore radius of mats formed from a large variety of fibrous filter aids. These filtrations were performed at the same pressure drop across the mat, but there was no indication of how the fluid velocities and mat thicknesses varied; and these two variables should both greatly affect retention.

Ghosh (27) and Eliassen (28) both studied the clarification of water with sand bed filters, and found that there was always penetration of some of the fine particles through the beds, and that the amount of material retained was always greatest in upstream sections of the bed and decreased toward the downstream side of the bed.

In contrast to solution clarification, a great deal of experimental work has been done in the field of aerosol filtration. However,

very little of this work has been carried out using well-defined systems with the objective of evaluating the mechanisms by which collection of the particles takes place.

Thomas and Yoder (15) have studied the penetration of dioctyl-phthalate aerosols through a column of lead shot. When they reversed the direction of flow from vertically down to vertically up, they noticed an increase in the amount of particles passing through the column uncollected. This data was obtained in the region where the diffusion and flow-line interception mechanisms were controlling. The increase in penetration can be attributed to the influence of the settling mechanism.

Wong (10) studied the removal of aerosol particles from high velocity air by the internal structure of high porosity glass fiber mats. In his system, inertial impaction was the controlling mechanism of retention even at Reynolds numbers below one. His data indicated that inertial impaction was not a significant mechanism of retention below a  $\psi$  value of about 0.6.

Marshall (18) studied the collection of a dye aerosol by wire screens. Thomas (17) studied the collection of a dye aerosol by glass fiber mats. Their data indicate that, by changing only the velocity, they went from a region where diffusion was the controlling mechanism of collection, to a region where the inertial impaction mechanism was controlling.

Humphrey (19) has studied the collection of bacteria spores from air by glass fiber mats. His data covered a range of velocities from the point where the diffusion mechanism was controlling to the point where the inertial impaction mechanism was controlling.

#### SUMMARY AND EXPERIMENTAL APPROACH

The removal of particles from a liquid by filtration falls into one of two types: cake filtration, or solution clarification. In the first, the particles are retained on the surface of the filter media, while in the second, they are retained by the internal structure of the media.

The phenomenon of solution clarification is very poorly understood, and a knowledge of the mechanisms by which a particle can move across the streamlines to collide with a fiber in a fibrous filter is essential to the eventual understanding of the retention of filler materials in the papermaking process.

It was pointed out that a rigorous theoretical solution of the problem of retention of fine particles by a fibrous structure was not possible.

In the field of aerosol filtration, eight mechanisms by which particles can be collected by solid surfaces have been demonstrated. Four of these were probable mechanisms by which particles could be removed from a liquid by the internal structure of a fibrous filter: inertial impaction, flow-line interception, Brownian diffusion, and settling.

If a fibrous mat is made up of cylindrical fibers, all lying in the X-Y plane, consideration of the flow pattern around the fibers as being similar to the flow pattern around an infinite cylinder in an infinite medium yields further information. Four dimensionless parameters have been related theoretically and experimentally to the collection of particles by the four mechanisms mentioned above.

This study was made with mats of cylindrical fibers in which the fibers were randomly oriented in the X-Y plane and approximately perpendicular to the direction of flow. The mats were compacted with a permeable piston to give them a uniform porosity. A dilute suspension of particles was then flowed through the mat at constant velocity, and the amount retained was determined.

The effects of three main variables (the fluid velocity, the fiber diameter, and the mat porosity) on the retention of particles by a fibrous mat were investigated.

## EXPERIMENTAL

### APPARATUS

A picture of the assembled apparatus is shown in Fig. 7. A piping diagram showing the path of the suspension through the apparatus is shown in Fig. 8.

The water used for suspending the fibers and particles was deaerated by boiling and cooling in a 50-gallon stainless steel tank with a conical bottom, which was located on the floor above the rest of the apparatus. Heating and cooling were accomplished with a copper coil, through which either steam or cold water could be passed. Agitation was accomplished with a 1/8-horsepower, variable-speed Lightnin' mixer equipped with a stainless steel shaft and propeller.

The slurry flowed out of the bottom of the tank through a half-inch rubber tube into the head chamber of the flow tube. A compressor clamp was used to control the flow rate into the head chamber. In addition, a float-operated solenoid was used to pinch off the rubber tubing when the level of the slurry in the head tube became too high. This was very useful at low flow rates, when the run times approached two hours.

The flow tube was made of Lucite, three-inch inside diameter, one quarter-inch wall thickness. The area available for flow was 45.3 square centimeters. Lucite was chosen because it would allow the mat formation process to be watched closely.

The flow tube was also fitted with pressure taps to permit the eventual observation of the pressure drop distribution in thick mats.

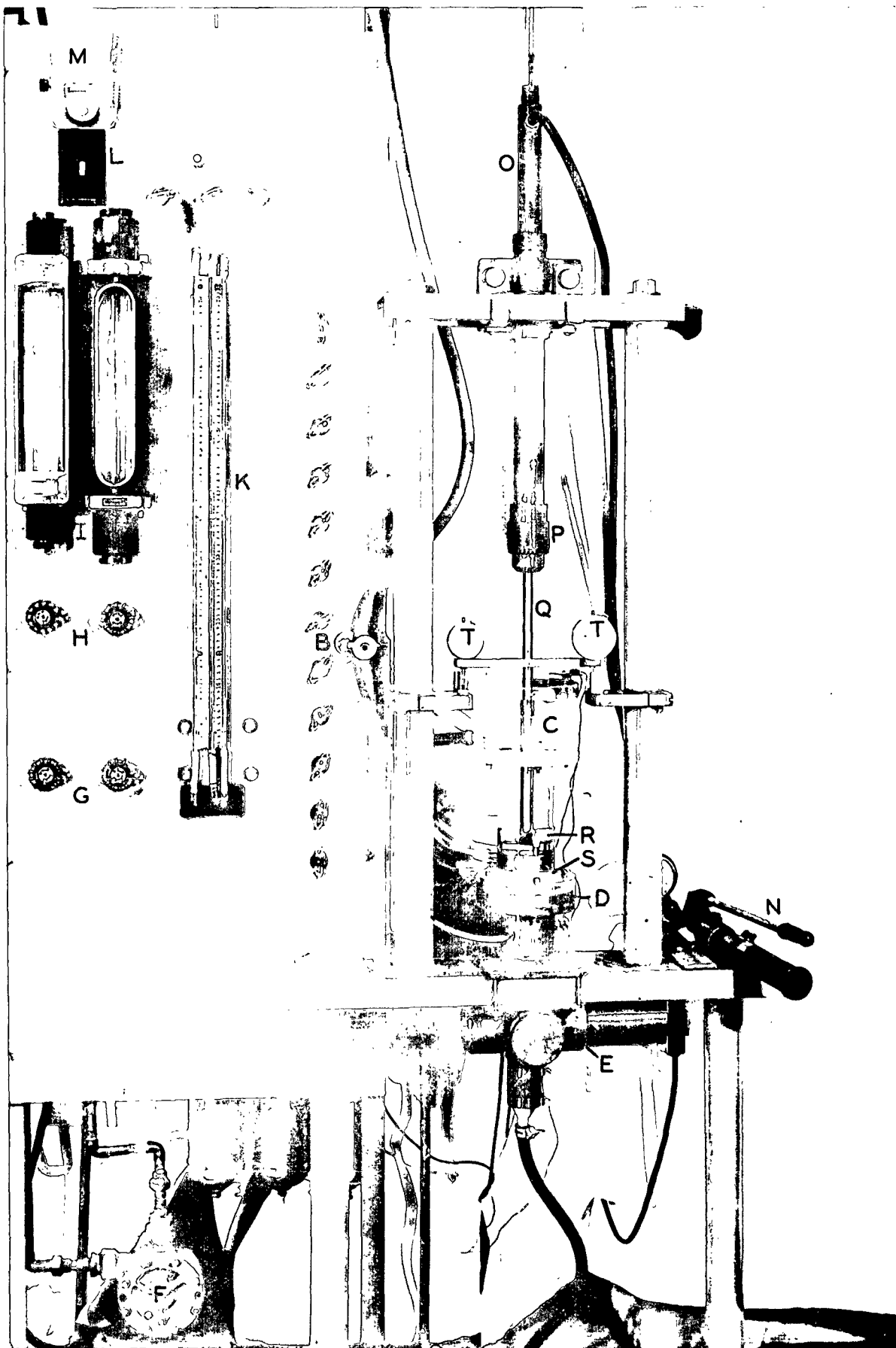
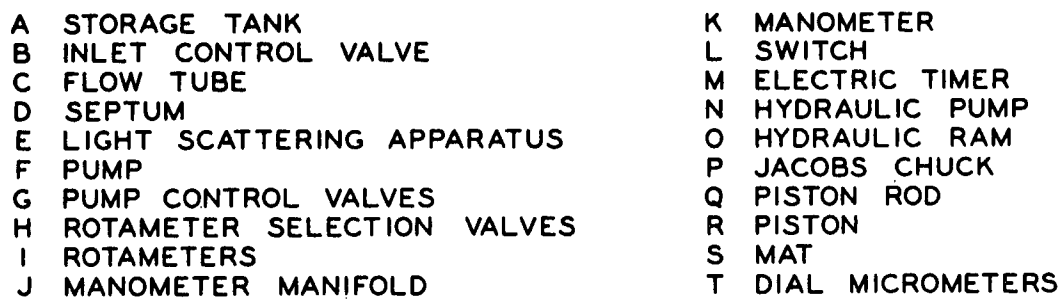


Figure 7. Photograph of Apparatus



SYMBOLS FOR FIG. 7 AND 8

Figure 8. Piping Diagram



The septum was made from one-inch brass plate. The edges were recessed on both the top and bottom, so that the area available for flow fit snugly up into the flow tube and down into the septum base. This greatly simplified alignment of the apparatus during assembly prior to each mat formation. The permeable piston was also made from a one-inch brass plate. Both the piston and the septum were drilled with 1/4-inch holes on 5/16-inch centers in an equilateral triangular pattern. Where this pattern did not come close to the edge of the area available for flow, additional smaller holes were drilled. All the holes were countersunk on the upstream side of the septum and the downstream side of the piston 1/32-inch deep with a 60° included angle countersink. Single 35-mesh stainless steel screens were soldered to the upstream face of the septum, and to the downstream face of the permeable piston, using a 1/16-inch ring of solder around the edge of the area available for flow. The 35-mesh stainless steel screen was chosen to give the best combination of:

1. A small amount of deflection of the surface of the pad into the openings of the screen, i.e., good definition of mat thickness.
2. A small amount of deflection of the screen under load into the holes drilled into the plate.
3. A minimum amount of surface for particles to deposit on.

The drilled holes on the upstream surface of the permeable piston were countersunk to minimize the flat area available for particles to settle out on. A photograph showing the details of construction of the permeable piston is shown in Fig. 9.

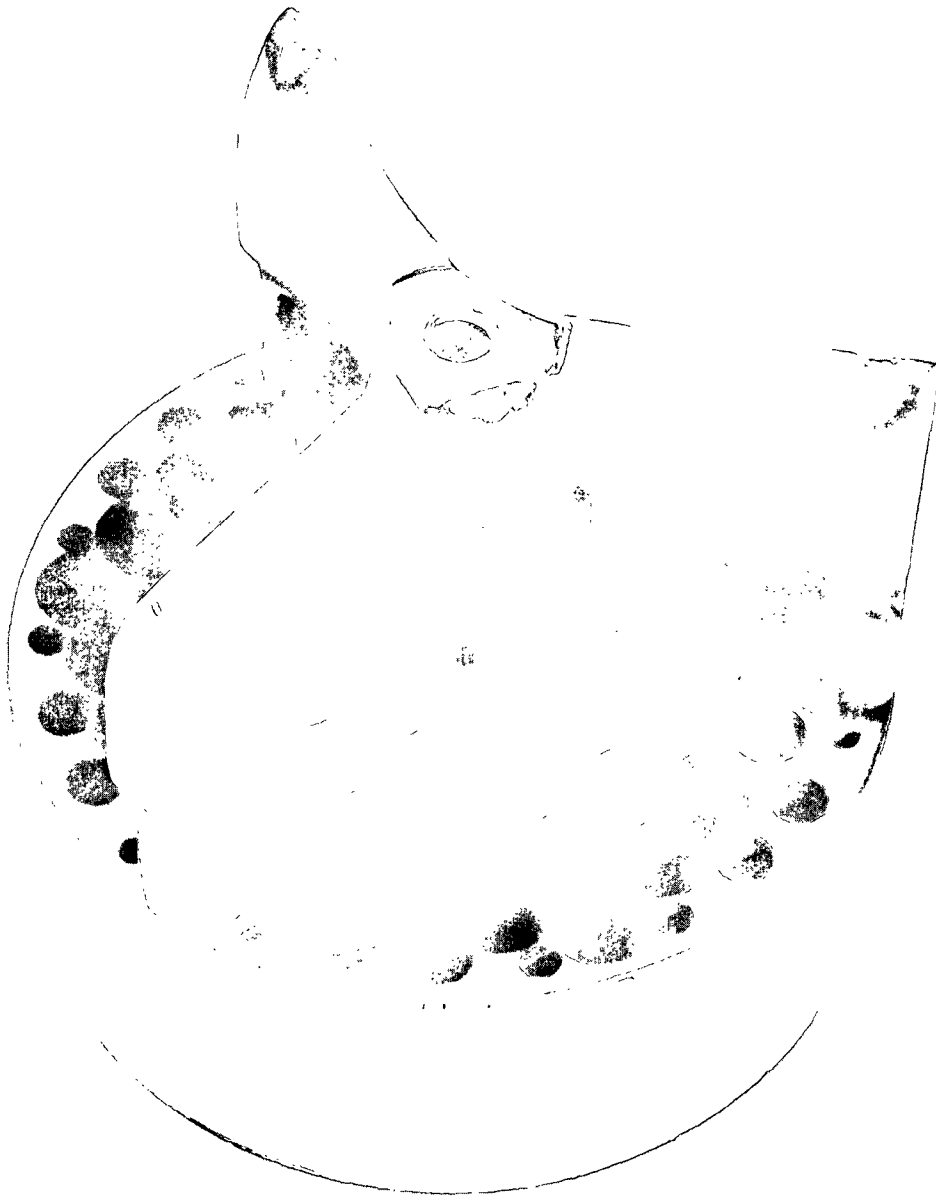


Figure 9. Photograph Showing Details  
of Construction of Permeable Piston

The mat thickness was measured by two dial micrometers mounted on the shaft of the piston.

A hydraulic pump and ram were used to force the shaft of the piston down to compact the mat. When the mat had been compressed to the desired thickness, the piston was locked in place by tightening a Jacobs chuck around the shaft of the piston.

The liquid that passes through the septum passes through the light-scattering apparatus, and then goes to the pump. A Roth turbine pump, type 020, rated at 0.8 g.p.m. at 100 feet of head, driven by a 1/4-horsepower, 1,750 r.p.m. motor, was used to draw the liquid through the mat and then force it through the rotameters to the sewer. The pump output was controlled by two needle valves; one was used to throttle the pump discharge, and the other was used to bleed some of the liquid discharge by the pump back into the intake. This permitted excellent control of the flow rate over the range of flow rates used.

The liquid discharged from the pump was passed through one of two Fischer-Porter rotameters to measure the flow rate. With the pump mentioned and the two rotameters, a flow rate range of 5.2 to 157 cc. per second was possible. This corresponded to a range of superficial velocities in the flow tube of 0.11 to 3.47 centimeters per second.

A series of three well-type differential manometers was used to measure the pressure drop across the mat. The manometers were made of uniform bore capillary tubing having an inside diameter of 0.04 inch. This small diameter was chosen to reduce the disturbance of the flow

pattern in the mat when liquid flowed horizontally into the pressure tap and then into the manometer system. The three manometer fluids used were tetrabromoethane, carbon tetrachloride, and chlorobenzene. One centimeter of liquid pressure drop on these manometers was then equal to 1.956, 0.588, and 0.103 centimeters of water, respectively.

A block diagram of the light-scattering apparatus is shown in Fig. 10. A Sorenson voltage regulator was used to provide a constant voltage source for the amplifier and the lamp. The output voltage of the Sorenson regulator was reduced to six volts with a transformer to operate the 50-candlepower light source. The light was focused into a slightly converging beam that passed horizontally through the center of the vertical glass pipe. The glass pipe had an inside diameter of 1-9/16 inches, and all liquid that had passed through the mat passed through the glass pipe. The light that was scattered at 90° to the incident beam passed through a copper sulfate filter\*, and was focused on the photocell of the Densichron probe. The signal generated in the probe unit was amplified with a Densichron AC Amplifier, and recorded on an Esterline-Angus strip chart recorder.

## MATERIALS

### FIBERS

In keeping with the use of a well-defined system in this study, the following properties of the fibers were required:

---

\*The photocell used was only sensitive to light in the blue end of the spectrum. However, exposure to light in the red end of the spectrum continually decreased its sensitivity. The copper sulfate filter eliminated this problem.

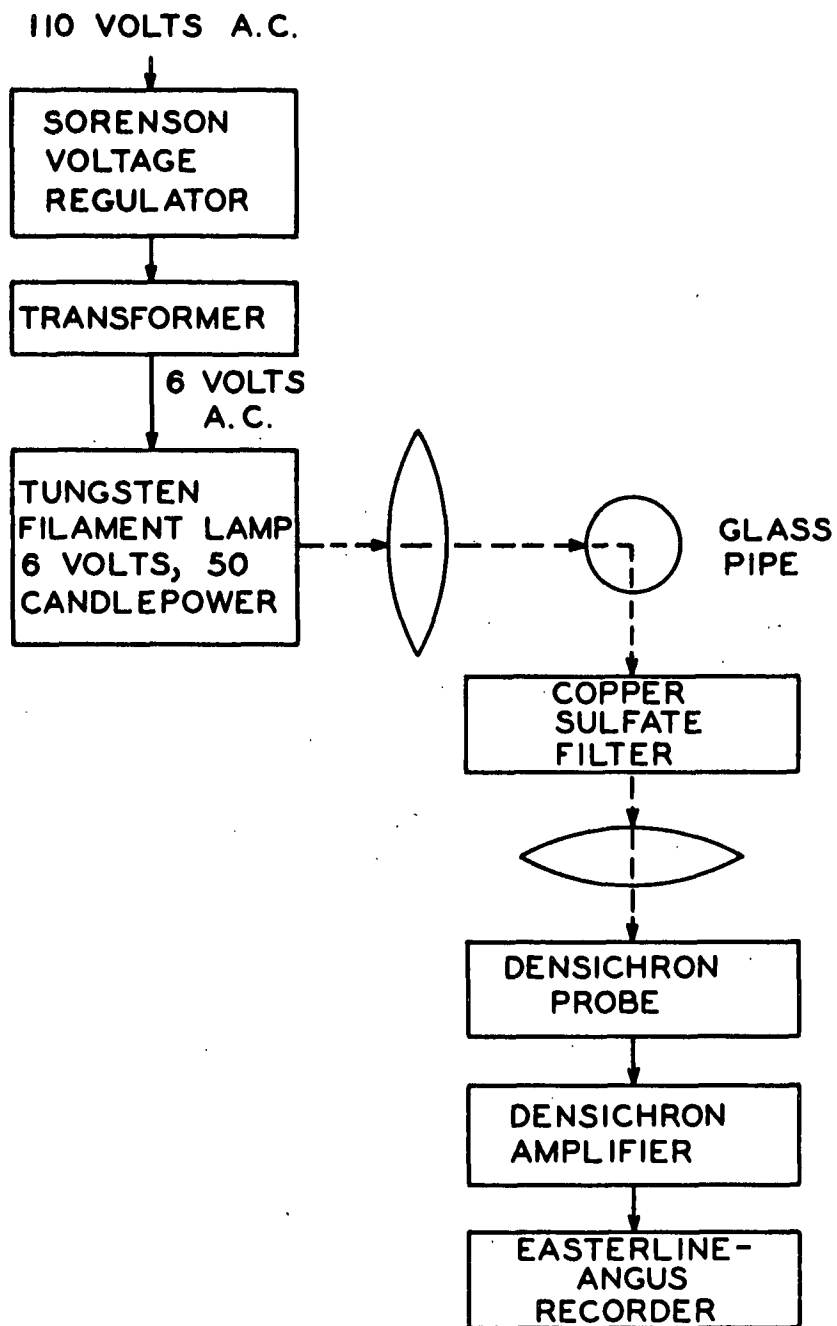


Figure 10. Block Diagram of Light-Scattering Apparatus

1. Cylindrical fibers having smooth surfaces.
2. Several samples having different fiber diameters.
3. A small distribution of diameters within each sample of fibers.
4. Easy dispersibility in water.
5. The fibers should be essentially nonswelling in water.

Nylon fibers obtained from E. I. du Pont de Nemours & Co., Inc., fulfilled all of the above requirements. All the fibers were obtained in the cut, "staple" form, except the 13.1-micron nylon fiber. This was obtained in continuous filament form and cut, using a special cutter consisting of a number of single-edge razor blades equally spaced with washers between them, and bolted rigidly together.

Photographs showing the cylindrical cross sections and smooth surfaces of the fibers are shown in Fig. 11 and 12. The properties of the fibers are summarized in Table I.

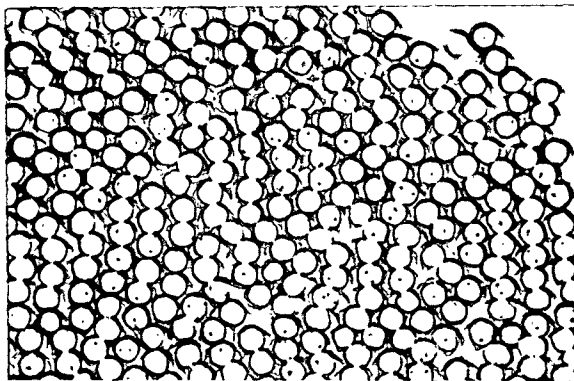
TABLE I

PROPERTIES OF NYLON FIBERS

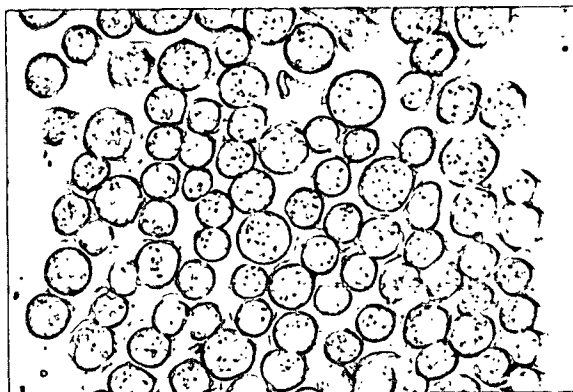
Av. Fiber Diam., $\mu$	Filament Denier	Fiber Length, in.	TiO <sub>2</sub> Content, %	Fiber Type
45.0	15	1/2	0.018	121
20.3	3	1/4	0.308	221
13.1	1.2	1/8	0.307	200

PARTICLES

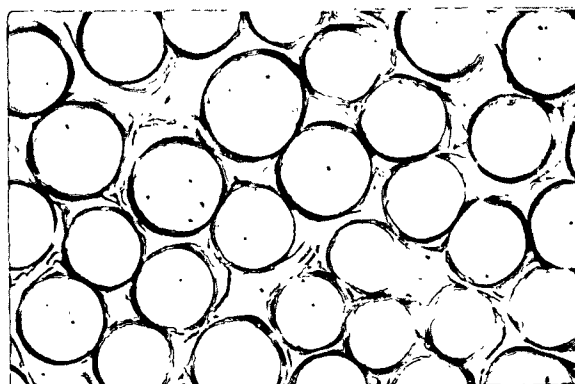
For this work, a spherical particle that could be characterized easily, and with the following properties, was desired:



13.1 Micron Fibers

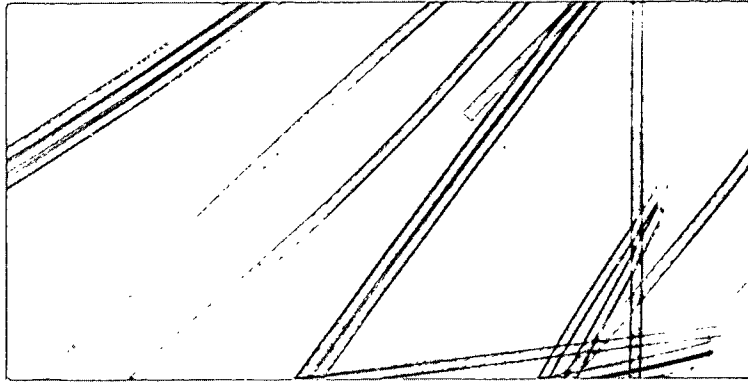


20.3 Micron Fibers

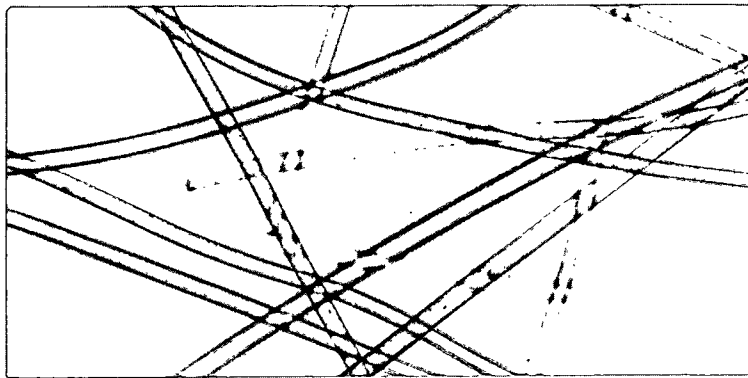


45.0 Micron Fibers

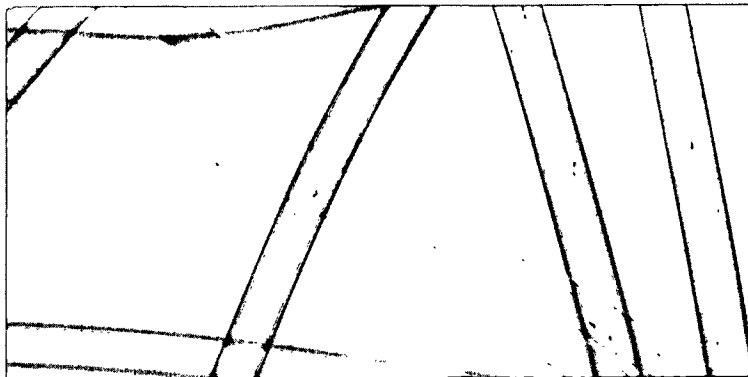
Figure 11. Photomicrographs Showing  
Cylindrical Cross Sections of Nylon  
Fibers. Magnification: 240X



13.1 Micron Fibers



20.3 Micron Fibers



45.0 Micron Fibers

Figure 12. Photomicrographs Showing  
Nylon Fibers as Smooth Cylinders  
Magnification: 120X



1. Average diameter between 1 and 10 microns.
2. Narrow diameter distribution.
3. The particles should be capable of easy dispersion to form a stable dispersion.
4. Quantitative analysis for a small amount of particles should be simple in the presence of large quantities of nylon.

Many different types of particles were examined, including carbonyl iron, glass beads, and precipitated calcium carbonate. Titanex RA50 was finally used. This was obtained from the Physical Chemistry Section of the Institute. As will be shown later, this material was not spherical, the average particle size was below one micron, and it did not have a very narrow size distribution.

Four hundred grams of titanium dioxide was dispersed at 70% solids in distilled water, using a combination of 1% Calgon T (sodium hexameta-phosphate) and 0.2% sodium carbonate as a dispersing agent. The dispersion was carried out in a Waring Blendor for one-half hour. The resultant slurry was diluted with distilled water to about 30% solids, and settled to remove any large agglomerates still remaining.\* After siphoning off the unsettled material, distilled water was added and the material was reslurried with a laboratory mixer and allowed to settle again. The unsettled material was siphoned off and the procedure was repeated once more.

---

\*It was assumed that free settling was taking place, Stokes' law held, and the effective density of the agglomerates was that of the single crystal. On this basis the material less than two microns in diameter was kept.

The dispersed slurry of titanium dioxide was stored in a tightly stoppered gallon jar. This jar was rotated continuously on a ball mill to prevent settling of the particles (there were no balls in the jar, so no further dispersion was taking place).

This material was used for several months in retention experiments, and the apparent particle size in the dilute slurry being filtered was about one micron. However, it was apparent that a better estimate of the particle size, and particle size distribution, was desirable.

Determination of the particle size of this material was difficult for several reasons. Although microscopic observation of the particles in water suspension using oil immersion optics and an eyepiece micrometer indicated an average particle size of about one micron, the Brownian motion of the particles was such that focusing on one particle long enough to make an accurate estimate of its size was almost impossible. Preliminary electron micrographs of the dispersed titanium dioxide indicated that agglomeration took place in the preparation of the grids that were observed. Therefore, electron micrographs could not be used to determine the size of the particles in this dispersion. However, the electron micrographs did indicate that the particles observed with the light microscope were actually loose agglomerates of very small particles. This information eliminated settling as a possible method of determining the particle size, because it required knowledge of the effective density of the agglomerates.

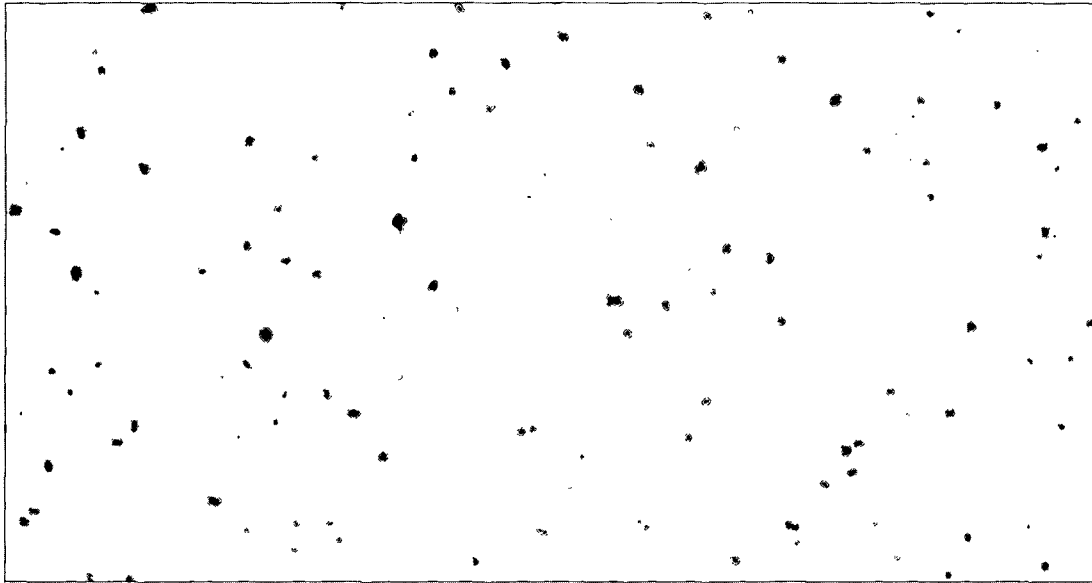
The particle size was finally determined by mixing a sample of the titanium dioxide dispersion with glycerin, to form an 80% glycerin suspension. The Brownian motion of the particles in microscope slides prepared from this mixture was small enough that photomicrographs could be taken, and the particles could be measured with an eyepiece micrometer in an optical microscope at 1000X. Measurement of over 900 particles showed a range of particle sizes from slightly less than 0.5 micron to slightly over 2 microns, with the bulk of the particles being about 1 micron. The number average diameter was 0.96 micron. A photomicrograph and an electron micrograph of the titanium dioxide particles used are shown in Fig. 13.

#### WATER

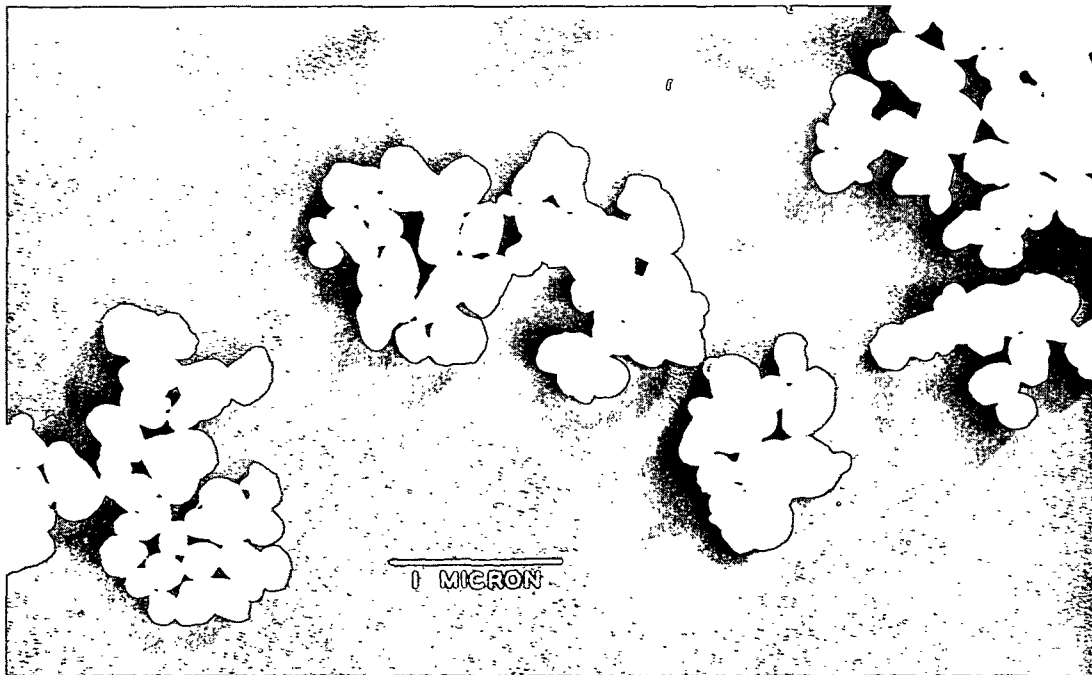
Large amounts of water were required for both the formation of the filter mat and for the filtration experiments. Five-gram mats of nylon fibers were used. This required about 100 liters of water to form the mats from an unflocculated suspension which would give the desired orientation of the fibers in the mat.

It was also felt that the stock suspension of titanium dioxide should be extensively diluted in the preparation of the suspension to be filtered in order to minimize agglomeration effects. A large volume of suspension also made control and measurement of the velocity of the suspension through the filter easier.

At first, it was thought that filtered and softened city water would be adequate for the filtration experiments. The retention of



Photomicrograph. Magnification: 1000X



Electron Micrograph. Magnification: 22,700X

Figure 13. Photomicrograph and Electron  
Micrograph of  $\text{TiO}_2$  Particles

titanium dioxide was essentially zero, and the results were very erratic. It was found that the pH of the city water was above 9, and it was suspected that the fibers and particles both carried a negative charge due to adsorbed hydroxyl ions. This would result in the fibers and particles repelling each other.

A long series of experiments\* were carried out which finally showed that the only suitable water for use in the filtration experiments in terms of reproducibility and assurance that electrostatic repulsion effects due to adsorbed ions were negligible was:

1. Water distilled from city water.
2. This was boiled and cooled to remove dissolved gases.
3. After the fibers or particles had been added, the pH was reduced to 4 with hydrochloric acid, and the ionic concentration was increased to  $5 \times 10^{-3}$  molar or above in calcium chloride.

Reduction of the pH to 4 reduced the hydroxyl ion concentration and therefore its preferential adsorption on the surfaces of the particles and fibers. In addition, under acidic conditions, the hexametaphosphate dispersing agent hydrolyses to the monophosphate, which is a much less effective dispersing agent.

Increasing the ionic concentration decreased the thickness of the electrical double layer. At a pH of 4, after the ionic concentration was increased above  $5 \times 10^{-3}$  molar in calcium chloride, the electrostatic repulsive forces due to adsorbed ions were always less than the

---

\*These experiments are discussed in Appendix I.

Van der Waal's attractive forces. This was indicated by the fact that, as the ionic concentration was increased from  $5 \times 10^{-3}$  to  $4 \times 10^{-2}$  molar in calcium chloride, the retention was constant at constant fiber size, velocity, and porosity. Extrapolation of Mossman and Mason's (29) and Harris and Sookne's (30) data also indicates that the electrical double layer would be collapsed under these conditions.

In all of the experimental work reported here, the fibers or particles were added to 105 liters of distilled water, and then 2 ml. of concentrated hydrochloric acid and 2 moles of calcium chloride dihydrate were added to produce the final suspension.

## PROCEDURES

### MAT FORMATION

An analytical balance was used to weigh out 5.00 grams of the desired diameter nylon fiber. This was carefully transferred to a clean filter flask, and a liter of boiling distilled water was added. The fibers were then deaerated under the vacuum produced by an aspirator.

The apparatus (flow tube, septum, and piston) was cleaned. The septum support, septum, and flow tube were bolted together. They were sealed with O-ring gaskets in grooves, and the bolts were tightened to the point where metal-to-metal and metal-to-Lucite contact occurred.

The piston was forced down against the septum and locked in place, and the dial micrometers were adjusted to zero. The piston was then removed from the flow tube. The septum was wet from below to remove any air bubbles under the screen, and the flow tube was filled with water.

The deaerated fibers were placed in the 105 liters of distilled water that had been boiled and cooled. They were dispersed with the stirrer, and 2 ml. of concentrated hydrochloric acid and two moles of calcium chloride dihydrate were added. This was thoroughly mixed into the suspension.

The mat was formed by filtration of this dilute suspension of fibers at a constant velocity of about 0.8 cm./sec. When the tank containing the fiber suspension was empty, the filtration process was stopped to prevent air from being drawn into the mat.

All the fibers remaining in the tank were carefully washed out, collected, dried, and weighed. This weight was subtracted from the dry weight of the fibers initially weighed out to obtain the weight of the fibers actually in the mat. This was used to calculate the required mat thickness for the desired porosity.

#### FILTRATION EXPERIMENT

The mat was compressed to the thickness required to obtain the desired porosity with the permeable piston and hydraulic ram.

Ten milliliters of the stock suspension of titanium dioxide (which was equivalent to 1.139 grams) were added slowly to 105 liters of distilled, deaerated water which had been cooled to 25°C. This was thoroughly mixed, 2 ml. of concentrated hydrochloric acid were added to reduce the pH to 4, and two moles of calcium chloride dihydrate were added. The resulting mixture was agitated for five minutes.

The valve that permitted the slurry to run into the flow tube was opened; the switch which turned on the pump, the electric timer, and the strip chart recorder for the light-scattering apparatus was closed. The flow rate was then quickly adjusted to the desired value.

At the end of the run, as the air-liquid interface approached the surface of the mat, the flow rate was reduced and the interface was pulled through slowly. This was done in an attempt to minimize the removal of particles from the fibers by surface tension effects. Light-scattering results and visual observation of the last slurry to pass through the mat indicated that no particles were removed.

The apparatus was disassembled and a small sample of the original slurry was poured into the glass pipe of the light-scattering apparatus. The light scattered by the original slurry then served as a reference point for the light scattered-time curve recorded on the Esterline-Angus recorder.

#### ANALYSIS

The filter mat was carefully removed from the flow tube and placed in a tared crucible. Any fibers that adhered to the septum or piston were carefully removed and washed into the crucible. The wet mat was then dried in an oven.

The mat was ashed very slowly in an electric furnace equipped with a temperature controller. The crucibles were heated rapidly to 600°F., and then the temperature was raised 50°F. per hour until it reached 900°F. After one hour at 900°F., the temperature was increased to 1200°F. and



held there for two hours. The crucible was then removed from the furnace and placed in a desiccator. The ashing procedure had to be carried out slowly, as the nylon first melted and then tended to foam. If the heating took place too quickly, the rate of foaming was greater than the rate of oxidation at the surface, and the material would foam over and down the edge of the crucible. To speed the oxidation, air was blown through the furnace at the rate of several cubic centimeters per minute.

The crucible and ash were weighed to determine the approximate amount of titanium dioxide present. This was used to determine the amount of reagents necessary to dissolve the material, and the size of the aliquot for the final titration.

The ash was carefully washed into a 500-ml. Erlenmeyer flask, and the water was removed by drying in an oven overnight.

A standard method for the analysis of titanium dioxide was used (16). Briefly, this consisted of the following steps:

1. Solution in boiling sulfuric acid, to which ammonium sulfate had been added to increase the boiling point.
2. Reduction of the  $Ti^{+4}$  to  $Ti^{+3}$  with aluminum metal.
3. Titration of the  $Ti^{+3}$  to  $Ti^{+4}$  with ferric ion under a carbon dioxide atmosphere.

Two modifications of the method were made:

1. One gram of aluminum did not always quantitatively reduce 0.2 gram of  $TiO_2$ , so two grams were used.
2. In the original method, the excess hydrogen generated was allowed to bubble through a sodium carbonate solution.

When the evolution of hydrogen ceased, the vacuum created sucked the sodium carbonate solution back into the flask. This reacted violently with the acid solution and created a carbon dioxide atmosphere over the solution. In the method as used, a stream of carbon dioxide gas was passed down into the flask after the evolution of hydrogen had almost stopped. This was continued as the solution was cooled before the titration.

## RESULTS AND DISCUSSION

### EFFECTIVE FIBER EFFICIENCY OF A CYLINDRICAL FIBER IN A MAT OF FIBERS

Since it is impossible to determine experimentally the amount of material collected by an individual fiber located in a mat of fibers, it is necessary to relate the entrance and exit particle concentrations to the effective collection efficiency of an individual fiber in the mat. This has been done by Wong (10); his derivation appears below:

Let  $\alpha$  = fiber volume per unit volume of mat, dimensionless

$\underline{h}$  = thickness of mat parallel to the direction of flow, cm.

$\underline{L}$  = length of fibers per unit volume of mat, cm.<sup>-2</sup>

$\underline{A}$  = face area of mat perpendicular to the direction of flow, sq. cm.

$\underline{N}$  = number of particles per unit volume of fluid, cm.<sup>-3</sup>

Now, by definition:

$$\alpha = \pi D_f^2 L/4 \quad \text{therefore} \quad L = 4\alpha/\pi D_f^2 \quad (10)$$

Assuming the mat to be uniform, the length of fibers which occupy the unit volume  $\underline{Adh}$  is  $\underline{LAdh}$ , and the projected area of the fibers perpendicular to the direction of flow in this volume is  $\underline{LAD_f dh}$ . The ratio of the number of particles collected by the fiber per unit time to the number of particles in the fluid stream passing through an area equal to the projected area of the fiber per unit time is equal to  $\eta$ , the effective fiber efficiency. Therefore, the fraction of the particles approaching the area  $\underline{A}$  which will be removed is  $\eta \underline{LAD_f dh/A}$ . Now, if  $\underline{N}$  is the number of particles per unit volume of fluid approaching the area  $\underline{A}$ , then:

$$- \Delta N = N \eta L A D_f dh/A \quad (11)$$

Substituting for  $\underline{L}$  and rearranging,

$$- \Delta N/N = \eta 4 \alpha dh/\pi D_f \quad (12)$$

Now, assuming that the number of particles removed per fiber layer is small and can be approximated by  $\underline{dN}$ , that the thickness of the mat is large compared to the thickness of a fiber layer, and that the amount removed per fiber layer is so small that good mixing takes place between each fiber layer, Equation (12) can be integrated between the limits of  $\underline{N} = \underline{N}_0$  to  $\underline{N}_h$  and  $\underline{h} = 0$  to  $\underline{h}$ , to give:

$$\ln (N_0/N_h) = 4 \alpha \eta h/\pi D_f \text{ or } \eta = \pi D_f \ln (N_0/N_h)/4 \alpha h \quad (13)$$

Equation (13) requires that  $\eta$  remain constant over the mat thickness. Marshall (18) and Thomas (17) have shown experimentally for the collection of a dye aerosol by a series of fine wire screens and a series of

thin glass fiber mats that  $\eta$  remains constant over the "mat" thickness. If  $\eta$  is constant over the mat thickness, then the logarithm of the fraction of particles penetrating the mat must be inversely proportional to the thickness of the mat. Humphrey (19) has shown this to be the case in the filtration of bacteria spores from air using a mat made of many thin fiber glass mats. His data covered the range of velocities from the point where the diffusion and settling mechanisms of collection were controlling to the point where the inertial impaction mechanism was controlling.

If one assumes that the particle diameter is constant, or that no fractionation of the suspended particles according to size takes place during the filtration, Equation (13) can be written as:

$$\eta = \pi D_f \ln (W_o/W_h) / 4\alpha h \quad (14)$$

where:

$\underline{W}_o$  = the mass of particles fed to the mat

$\underline{W}_h$  = the mass of particles passing through the mat =  $\underline{W}_o - \underline{W}_{mat}$

$\underline{W}_{mat}$  = the mass of particles retained in the mat

#### ASSUMPTIONS IN DERIVATION

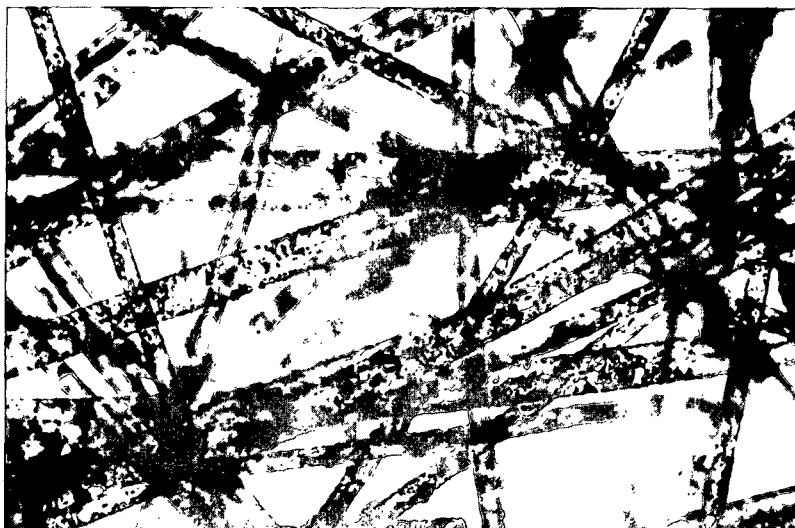
One of the assumptions in the derivation of Equation (14) is that there are no preferential areas for flow in the mat, i.e., no channeling. It was also assumed that the projected area of the fibers normal to the direction of flow was equal to the product of the total fiber length and the average diameter of the fibers. These assumptions require that the fibers all be in the X-Y plane perpendicular to the direction of flow.

Both of the above requirements were met in the method used in the mat formation. The absence of flocculation during formation was visibly evident. The fact that fiber mats formed could be delaminated into layers only several fibers in thickness was evidence that the fibers were essentially in the X-Y plane.

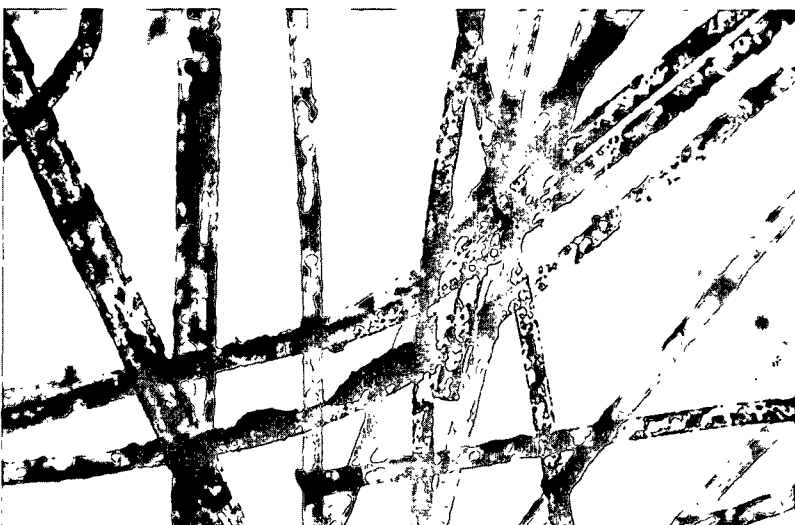
It might appear that the use of Equation (14) to analyze retention data in terms of the effective fiber efficiency would require the assumption that every particle that collided with a fiber adhered to it. Actually, it only requires that the fraction of fiber-particle collisions that result in adhesion be constant over the thickness of the mat, and for the thin mats used, this assumption does not appear unreasonable.

The derivation of Equation (14) suggests that the deposits of particles on the fibers will be uniform; or, if the deposition is actually according to a random process, that the thickness of the deposits on the fibers follows a normal distribution. However, the use of Equation (14) to analyze retention data only requires that the deposits on different fibers in the same fiber layer be similar.

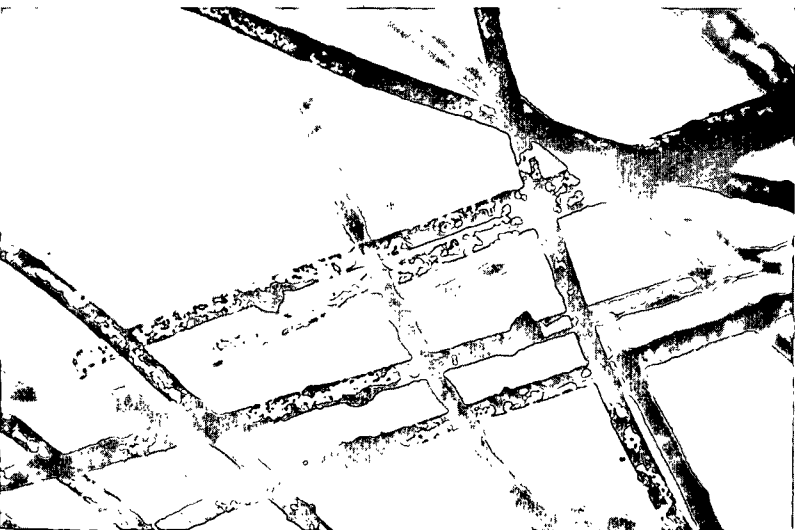
Photomicrographs of fibers taken from the top, middle, and bottom of a single filter mat are shown in Fig. 14. Additional photomicrographs of fibers taken from other fiber mats are shown in Fig. 15. The deposits on the fibers are definitely not uniform. Some areas of the fibers have a coating of particles many particles thick, while in some cases there are areas immediately adjacent that are completely barren of particles. Thus, the thickness of the deposits also does not follow



Bottom of Mat



Middle of Mat



Top of Mat

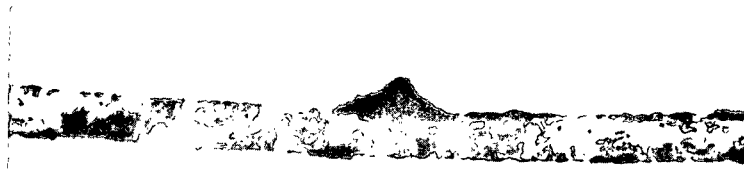
Figure 14. Photomicrographs Showing Similarity of Particle Deposits at Different Points in the Filter Mat  
13.1 Micron Fibers. Magnification: 200X

a normal distribution. However, the photomicrographs in Fig. 14 do show that the deposits on different fibers in the same fiber layer are similar in shape, size, and distribution. The deposits in different fiber layers are also shown to be similar in shape and distribution, though not in amount.

It was expected that the retention of particles by a given mat under given conditions would be constant from the beginning of the experimental filtration run until the end. The light-scattering apparatus, which measured the amount of light scattered by the particles that had passed through the mat, showed that this was not the case. The amount of particles passing through the mat was initially high, and then decreased with time, approaching a constant value. Grace (5) also observed the phenomenon of the retention increasing with time in his study of the filtration of carbonyl iron particles using various felts as the filter media.

A copy of a typical plot of light scattered by the particles passing through the mat is shown in Fig. 16. The straight line superimposed on the plot represents the light scattered by a sample of the original slurry. The ratio of the areas,  $I/(I + II)$ , is equal to the ratio of the weight of particles retained by the mat to the total weight of particles passed to the mat. This agreed with the results obtained by analysis of the titanium dioxide in the mat to within 10%.

The apparent maximum in the amount of particles passing through the mat is due to the fact that the flow tube is initially filled with water, and the light-scattering equipment is located an appreciable



13.1 Micron Fiber. Magnification: 450X



13.1 Micron Fiber. Magnification: 450X



45.0 Micron Fiber. Magnification: 450X



45.0 Micron Fiber. Magnification: 200X

Figure 15. Photomicrographs Showing  
Deposits of  $\text{TiO}_2$  Particles on Fibers  
from a Filter Mat



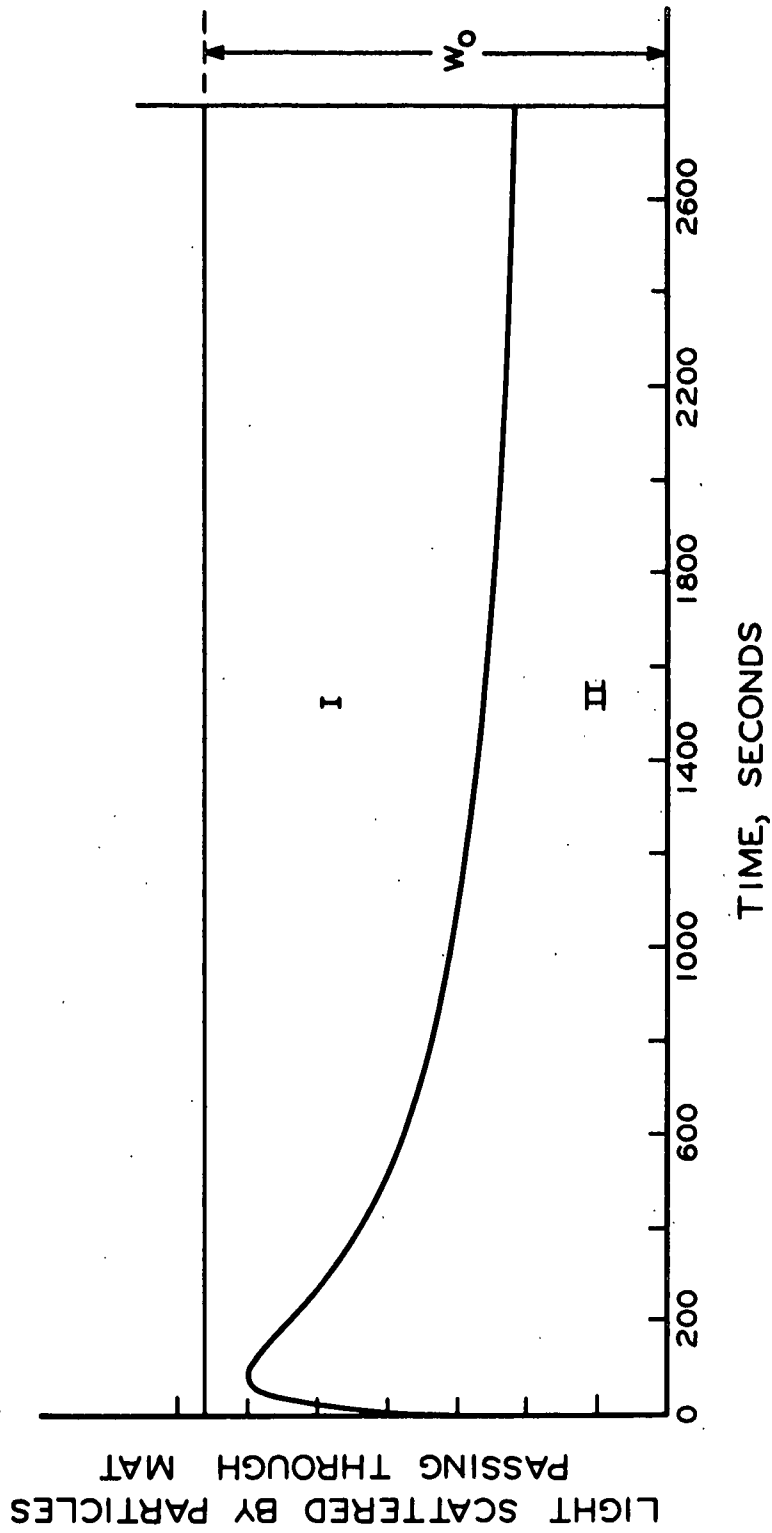


Figure 16. Typical Plot of Light Scattered by the Particles Passing Through the Mat Versus Time

distance below the bottom of the filter mat. Thus, mixing of the particle suspension and water takes place and the initial change in particle concentration at the point of measurement is gradual rather than abrupt.

The first particles retained by the fibers in the mat are probably retained by a purely random process. The presence of these particles on the surface of the fibers then alters the flow pattern around the fibers and the surface attractive forces. The probability of collection of the next particles flowing past the fiber is then increased, either by the alteration of the flow pattern near the particle already attached to the fiber, or by the presence of a higher attractive force between the particle in the suspension and the particle attached to the fiber than between the suspended particle and an adjacent bare area of the fiber. Thus, the deposits of particles tend to become very nonuniform, and the retention of particles increases with time. Haslam (21) observed the collection of zinc sulfide particles from a liquid flowing around a single fiber in a capillary tube. He also noticed that the particles tended to collect on particles already attached to the fiber, rather than bare areas of the fiber. If the particles collected by the fibers in the mat did not alter the flow pattern around fibers, there would be no change in the pressure drop from the beginning to the end of the run. A plot of the pressure drop across the mat as a function of time for run number 93 is plotted in Fig. 16A. (The data obtained from run number 93 was also used in plotting Fig. 16.) Retention of enough titanium dioxide to change the solid fraction only 3% resulted in a 65% increase in the pressure drop. This indicated that the presence of titanium dioxide

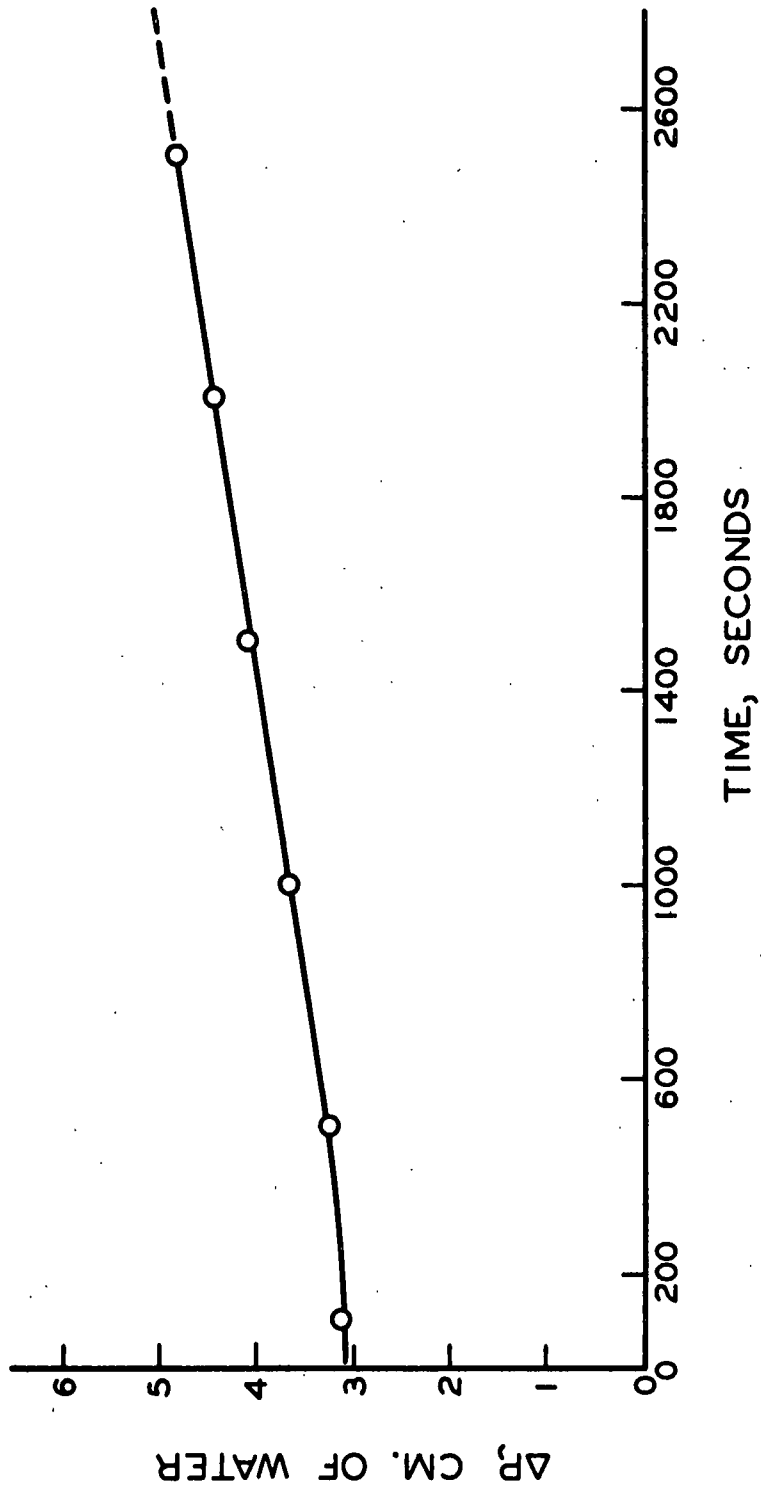


Figure 16A. Variation in the Pressure Drop  
Across the Mat With Time

particles on the surface of the fibers greatly influenced the flow pattern around the fibers.

It can be seen from Fig. 16 that the retention of titanium dioxide particles from water flowing through mats of nylon fibers used in this study was an unsteady state process. The retention was dependent not only on the fluid and mat properties, but also on the amount of titanium dioxide particles already in the mat.

The time required for a particle to pass through the mat was of the order of one second. Compared to this interval of time, the rate of change of the amount of particles being collected by the mat was small. Therefore, at any given point in time, the retention process in the mat can be approximated by a steady state process.

The light-scattering system used for obtaining the instantaneous retention data was not suitable for quantitative work, and determining the initial value of the effective fiber collection efficiency would have been very difficult experimentally. Therefore, since the shape of the instantaneous retention versus time curve was the same for all the experiments, the concentration and volume of the titanium dioxide suspension passed through the mat were held constant, and the retention data were analyzed using the amount of titanium dioxide retained in the mat at the end of the filtration experiment. Thus, the instantaneous retention was averaged over the filtration experiment and the unsteady state process was approximated by a steady state process in the analysis of the data.

## PRESENTATION AND ANALYSIS OF DATA

### DETERMINATION OF THE EFFECTIVE FIBER EFFICIENCY

If the retention of titanium dioxide particles by mats of nylon fibers is a random process, and the average effective fiber efficiency is constant from the top of the mat to the bottom of the mat, Equation (14) should fit the data.

$$\eta = \pi D_f \ln [W_o / (W_o - W_{mat})] / 4\alpha h \quad (14)$$

Therefore, if a single mat were sectioned at the end of a filtration experiment, and the sections were analyzed, a plot of  $\ln [W_o / (W_o - W_{mat})]$  versus  $h$  should yield a straight line passing through the origin. In a uniformly compacted mat, the mat weight  $W$  is directly proportional to  $h$  and is more easily determined for the sections than  $h$ . A plot of  $\log [W_o / (W_o - W_{mat})]$  versus  $W$  for two widely different mats is shown in Fig. 17. The data do indeed fall on a straight line which passes through the origin, indicating that  $\eta$  is constant from the top of the mat to the bottom.

### EFFECT OF FLUID VELOCITY AND FIBER DIAMETER ON $\eta$

The filtration experiments were carried out at six different superficial velocities, ranging from 0.39 to 3.09 cm./sec., and using three different diameters of nylon fibers, 13.1, 20.3, and 45.0  $\mu$ . A plot of  $\eta$  versus  $V_s$  with  $D_f$  as a parameter is shown in Fig. 18. The collection efficiency decreases with increasing velocity and increases tremendously with decreasing fiber diameter.

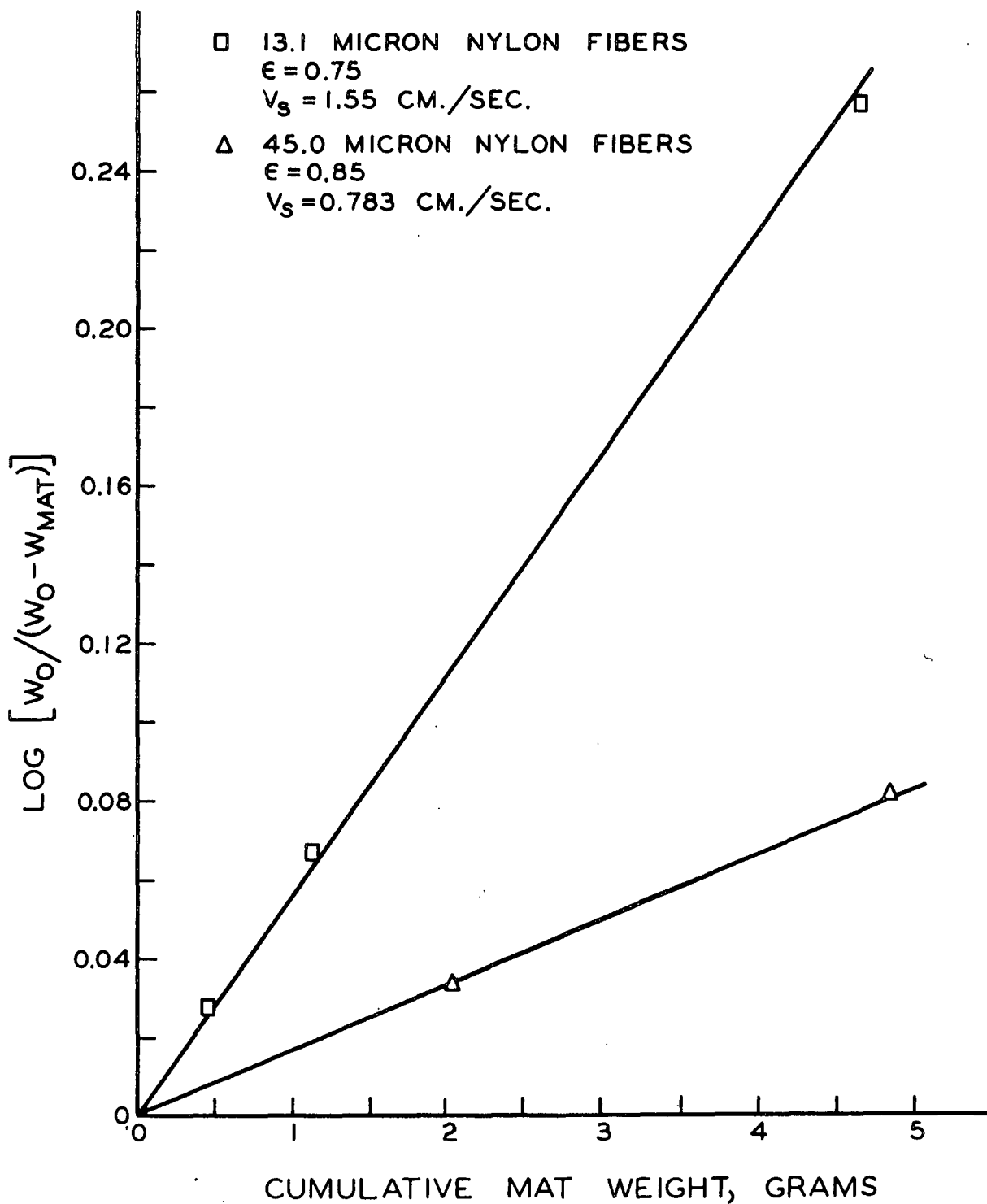


Figure 17. Data From Mat Sectioning Experiments

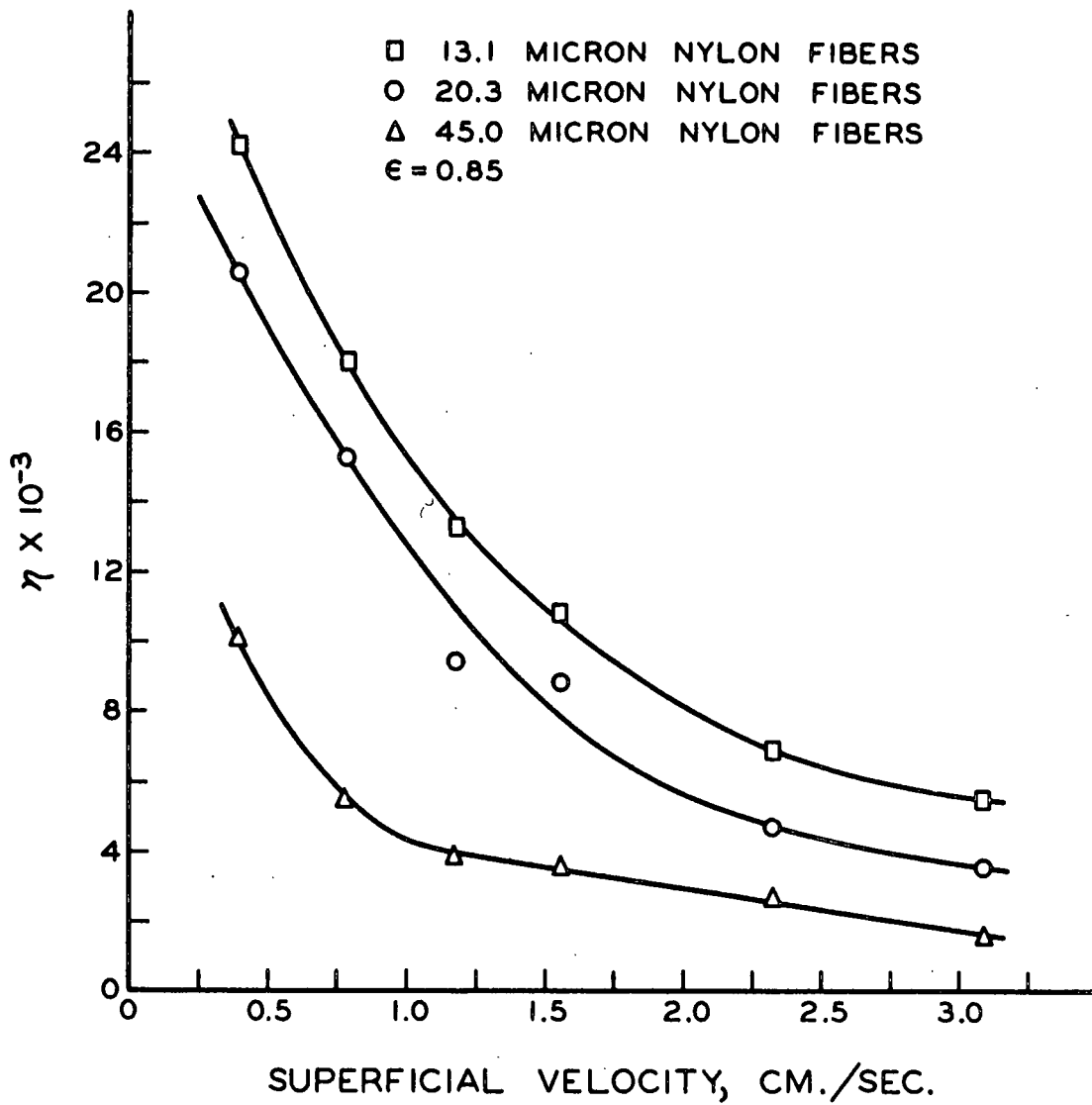


Figure 18. The Effect of Fluid Velocity and Fiber Diameter on  $\eta$

At the same velocity the flow pattern around different diameter cylinders will be different. The flow pattern around cylinders of various sizes will be the same at a constant Reynolds number. A Reynolds number for a cylindrical fiber in a fibrous mat was then defined as:  $Re = \rho \frac{V_s}{\mu} D_f$ . The data shown in Fig. 18, were then replotted in Fig. 19, as  $\eta$  versus  $Re$ . The data for the three different fiber diameters now all fitted one curve.

#### EFFECT OF MAT POROSITY ON $\eta$

The effect of the mat porosity on the effective fiber efficiency at constant superficial velocity should depend on the controlling mechanism of collection. When the porosity is decreased, the effective area available for flow decreases, and the average velocity in the mat increases at constant superficial velocity. Also, the movement of adjacent fibers closer together will increase the curvature of the streamlines around the fibers. Therefore, the effective fiber efficiency should increase with decreasing porosity if the inertial impaction or flow-line interception mechanisms of collection were controlling. If diffusion were the controlling mechanism, the effective fiber efficiency should increase due to the fact that more particles are passing closer to the fiber, but should decrease because the velocity close to the fiber surface is increasing and reducing the time for diffusion to take place. Chen (26) found in the filtration of an aerosol at constant superficial velocity where the diffusion mechanism of collection was apparently controlling that the effective fiber efficiency increased with decreasing porosity. The range of porosities used was from 0.90 to 0.99.



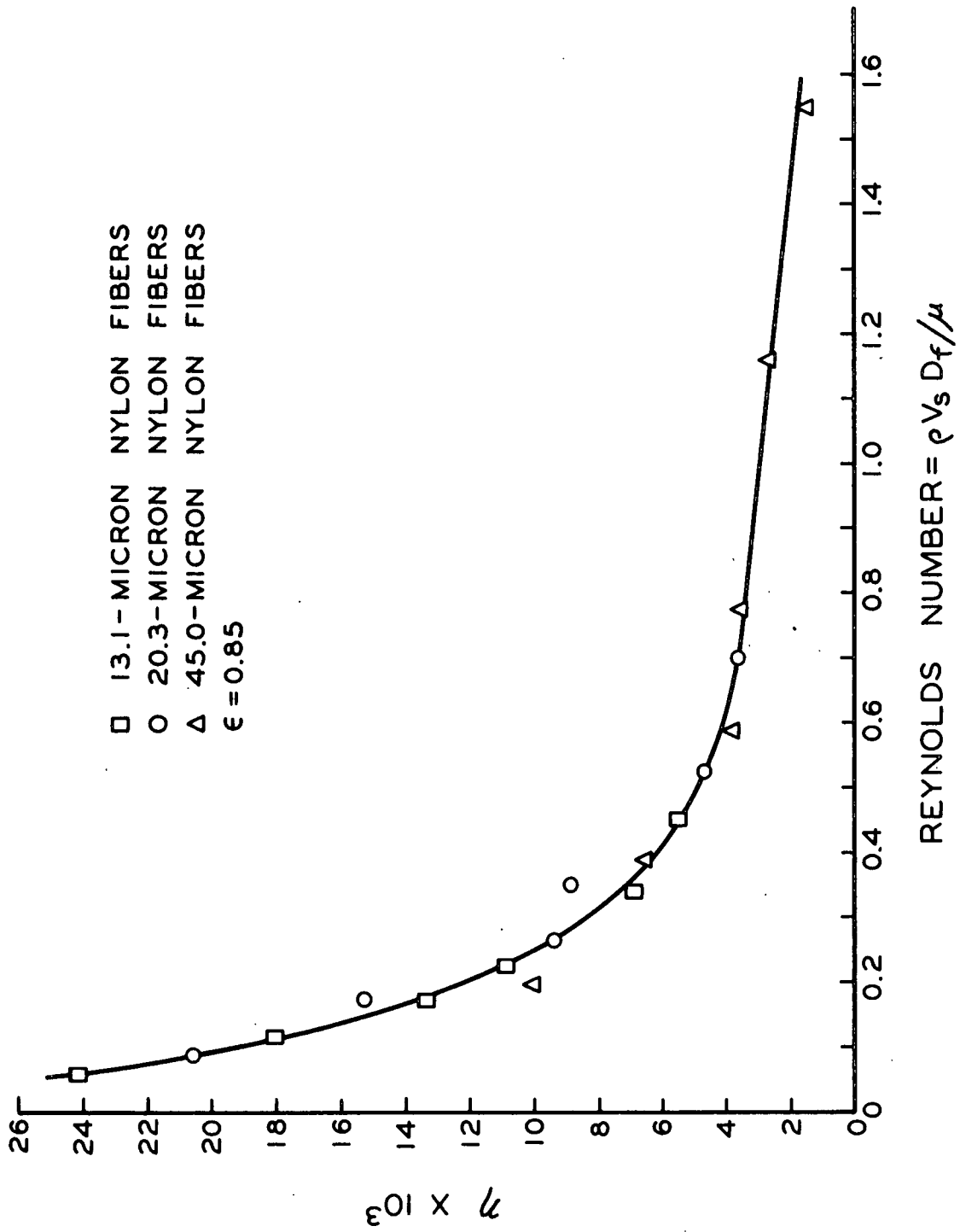


Figure 19.  $\eta$  As a Function of Reynolds Number

Most of the filtration experiments in this study were made at a constant porosity of 0.85. Several experiments were made at porosities of 0.75 and 0.90 to check the effect of mat porosity on the effective fiber collection efficiency. The results of this work are shown in a plot of  $\eta$  versus  $Re$ , with the porosity,  $\epsilon$ , as a parameter in Fig. 20. This method of plotting results in a family of curves, with a lower value of  $\eta$  at lower porosities. This can be explained by the fact that the average velocity in the mat is not the superficial velocity. The actual area available for flow is reduced by the presence of the fibers. Therefore, the actual average velocity in the mat is closer to  $\frac{V_s}{\epsilon}$  than  $\frac{V_s}{\epsilon}$ . Plotting  $\eta$  versus the Reynolds number defined as  $Re' = \rho \frac{V_s}{\epsilon} \frac{D_f}{\mu \epsilon}$ , should reduce the family of curves in Fig. 20 to a single curve if the interference of adjacent fibers in the flow pattern has not changed appreciably due to the fibers having been moved closer together. This is shown to be the case in the upper curve of Fig. 20.

The discrepancy at the porosity 0.9 is probably due to scatter in the data. It can be seen in Fig. 22, and in Appendix II, that occasional values of  $\eta$  were as much as 20% higher or lower than the expected value.

The range of porosities investigated is very small for two reasons. To compress the mat to a porosity of 0.7 would have required a load of 490 pounds on the piston assembly, which might have permanently deformed the upper part of the piston. At porosities above 0.9, the fluid drag force on the fibers becomes important. The force on any one layer of fibers in the mat is the sum of the fluid drag force on all of the fiber layers above it. This results in a nonuniform porosity when thick mats

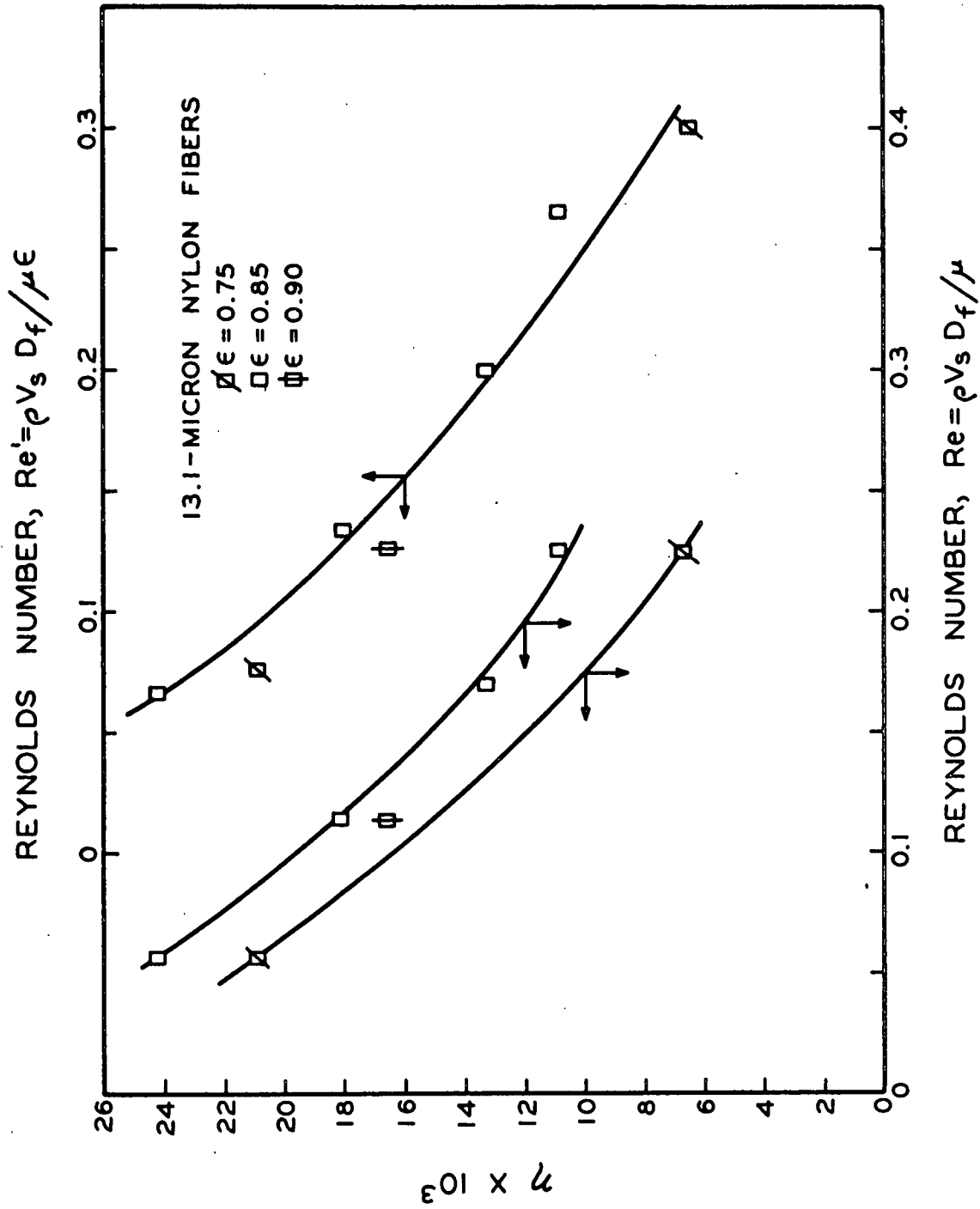


Figure 20. Effect of Porosity on  $\eta$

are used, and for very thin mats, the possible error in the measurement of the mat weight and thickness become large.

#### PROBABLE CONTROLLING MECHANISM OF COLLECTION

As stated before, the probable mechanisms of retention operating in the collection of titanium dioxide from water by mats of nylon fibers are sieving, settling, flow-line interception, inertial impaction, and Brownian diffusion.

Sieving can be definitely discarded as the controlling mechanism of retention. The pictures of the fibers taken from a fiber mat show that the interfiber spacings are much larger than the particles. Also, retention by sieving should not be velocity dependent. Further, at constant velocity,  $\eta$  should increase with decreasing porosity if sieving were important, and the reverse actually happened.

It is doubtful that settling is the controlling mechanism of retention, because the ratio of the free settling velocity to the superficial velocity,  $\frac{V_g}{V_s}$ , is so low. Assuming that the bulk density of the titanium dioxide agglomerate is the same as the density of a single crystal, and that the drag force on the irregularly shaped particle is the same as on a sphere, the settling velocity according to Stokes' law for a one-micron titanium dioxide particle is about  $2 \times 10^{-4}$  cm./sec. (The actual settling velocity will be somewhat lower than this, because of the above assumptions.) Therefore, the ratio,  $\frac{V_g}{V_s}$ , at the lowest velocity used is about  $5 \times 10^{-4}$ .

Thomas and Yoder (15) found that, in the filtration of an aerosol with a column of lead shot, settling became a significant mechanism of collection at ratios of  $\frac{V_g}{V_s}$  over about  $4 \times 10^{-5}$ . Their system was very different from the system used in this study, so that a direct comparison is not possible. However, their data do indicate that settling may be a significant mechanism of collection when the free settling velocity is still very small compared to the superficial velocity.

Langmuir's equation predicting the variation in  $\eta_0$  with fiber diameter when the flow-line interception mechanism is controlling [Equation (2)], indicates that  $\eta$  should increase drastically as the fiber diameter is decreased at constant Reynolds number. Actually, it remained constant, indicating that flow-line interception is not the controlling mechanism of collection.

Wong (10) has studied the filtration of aerosols in the region where inertial impaction was the controlling mechanism of collection. He found that inertial impaction was an important mechanism of collection only above a value of  $\psi$  equal to 0.6. Above this value,  $\eta$  increased rapidly as the velocity increased. In this study, the highest value of  $\psi$  was equal to  $4.7 \times 10^{-4}$ , and  $\eta$  always decreased with increasing velocity. Therefore, inertial impaction could not be the controlling mechanism.

Langmuir's equation predicting the variation in  $\eta_0$  with velocity when the diffusion mechanism is controlling [Equation (6)] indicates that  $\eta$  should decrease with increasing velocity, which is what occurred

in this study. Therefore, it appears that diffusion is the controlling mechanism of retention.

#### CONFIRMATION OF BROWNIAN DIFFUSION AS CONTROLLING MECHANISM OF RETENTION

Brownian diffusion appeared to be the controlling mechanism of retention, but at this point it seemed desirable to introduce another variable, which would greatly affect the diffusion mechanism, and therefore the collection efficiency if Brownian diffusion were the controlling mechanism of collection. The diffusion coefficient was the variable chosen.

Einstein (22) has shown the effective diffusion coefficient for a particle in a liquid to be:

$$D_{BM} = kT/3\pi \mu D_p \quad (3)$$

The most logical way to change the diffusion coefficient would have been to change the size of the particles being used. However, this is complicated by the fact that, in this particular size range, the accurate determination of particle size is very difficult.

A different fluid of a greatly different viscosity could have been used, but this would have been complicated by a lack of knowledge about fiber swelling and effects due to adsorbed ions or molecules.

By increasing the temperature of the system from 25 to 50°C., the diffusion coefficient could be increased from  $5.08 \times 10^{-9}$  to  $8.98 \times 10^{-9}$  sq. cm./sec. The large decrease in viscosity with increasing temperature

meant that the retention results could not be compared to constant velocity, but had to be compared to constant Reynolds number, so that the flow patterns around the fibers would be comparable. Therefore, at constant Reynolds number, a significant increase in  $\eta$  with an increase in the temperature of the system (which results in a higher diffusion coefficient) could be attributed to the diffusion mechanism of collection, and would indicate that diffusion was the controlling mechanism of collection in this study. The high temperature data are shown with the low temperature data in a plot of  $\eta$  versus  $Re'$  in Fig. 21. All the data support the conclusion that Brownian diffusion was the controlling mechanism of collection over the range of variables investigated in this study.

However, it should be pointed out that, in comparing the data at constant Reynolds number, the ratio of  $\frac{V_g}{V_s}$  increases with increasing temperature proportional to  $(\mu_{25^\circ C.}/\mu_{50^\circ C.})^2$ . Therefore, if settling were the controlling mechanism of collection,  $\eta$  would also increase with increasing temperature.

#### FINAL CORRELATION OF DATA

Figure 21, suggests that all the data presented thus far could be brought together into one correlation. Langmuir's equation predicting the collection efficiency of a single cylinder in an infinite medium where Brownian diffusion is the only mechanism of collection suggests a correlation of the form:

$$\eta = a(Re')^b(Sc)^c \quad (15)$$

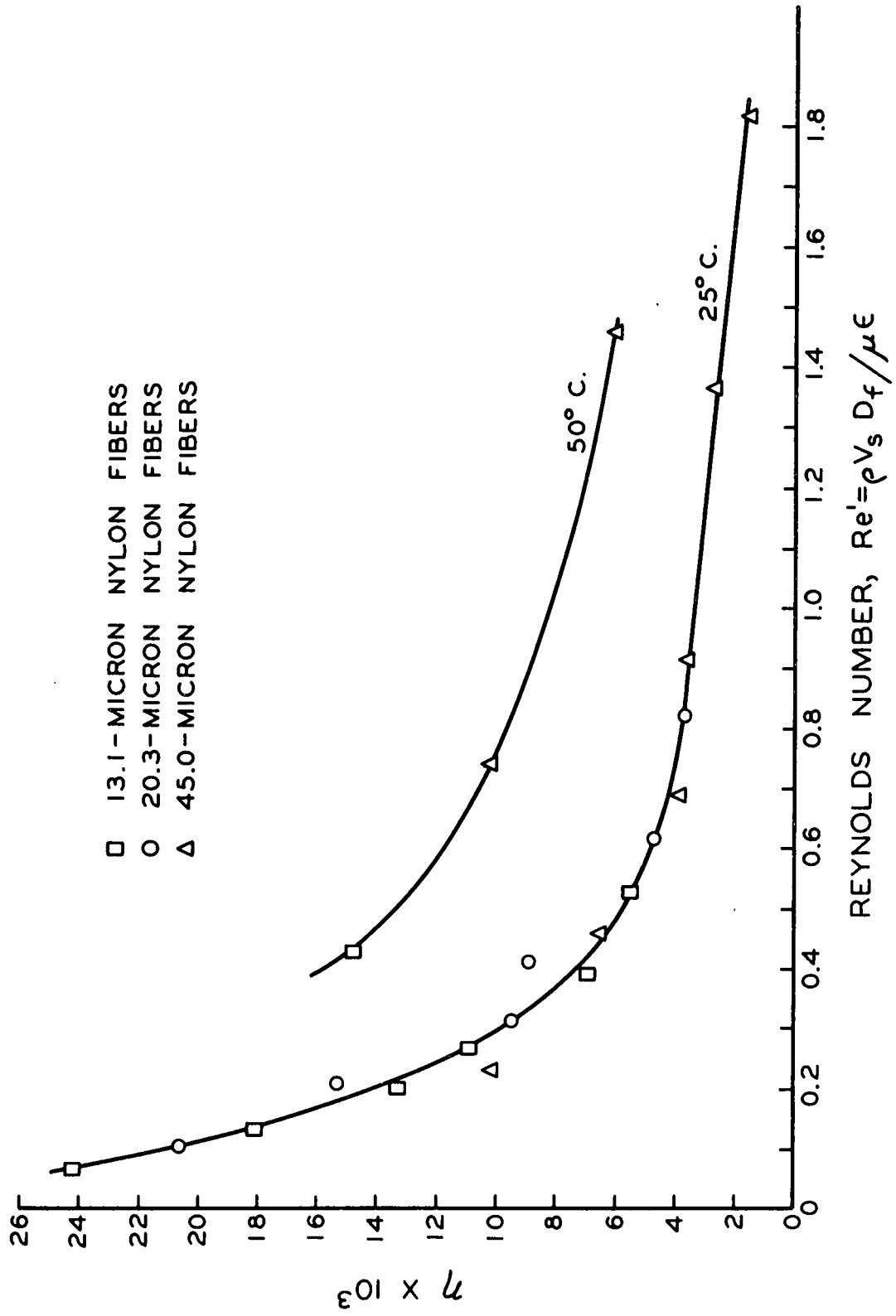


Figure 21. Effect of Temperature on  $\eta$



where a, b, and c are constants. This form is also suggested by data on heat and mass transfer from single cylinders to flowing fluids where molecular diffusion is the controlling mechanism of transfer (23).

When the logarithm is taken of both sides of Equation (15), it becomes:

$$\log \eta = \log a + b \log (\text{Re}') + c \log (\text{Sc}) \quad (16)$$

Therefore, when the data are plotted in the form of  $\log \eta$  versus  $\log \text{Re}'$ , it should fall about two parallel straight lines, with the high-temperature data being above the low temperature data. The data are shown in this form in Fig. 22, and the data are scattered about two straight lines that are approximately parallel.

Statistical treatment of these data shows that the equations of best fit are:  $\log \eta = -2.480 - 0.833 \log (\text{Re}')$  for the low-temperature data, and  $\log \eta = -2.095 - 0.746 \log (\text{Re}')$  for the high-temperature data. The 95% confidence limits on the exponent of the Reynolds number for the low-temperature data are from -0.725 to -0.927. This indicates that the exponents of the Reynolds number for the high- and low-temperature data are not statistically different. Assuming the exponent -0.83 is correct, the values of a and c for the correlation can be calculated. The value of the exponent c is -0.83, with the 95% confidence limits being from -0.52 to -1.08. The value for the constant a is equal to -2.64, with the 95% confidence limits being from -2.50 to -2.78. Therefore, the equation of best fit of the data is:

$$\eta = 2.29 \times 10^{-3} (\text{Re}')^{-0.83} (\text{Sc})^{-0.83} \quad (17)$$

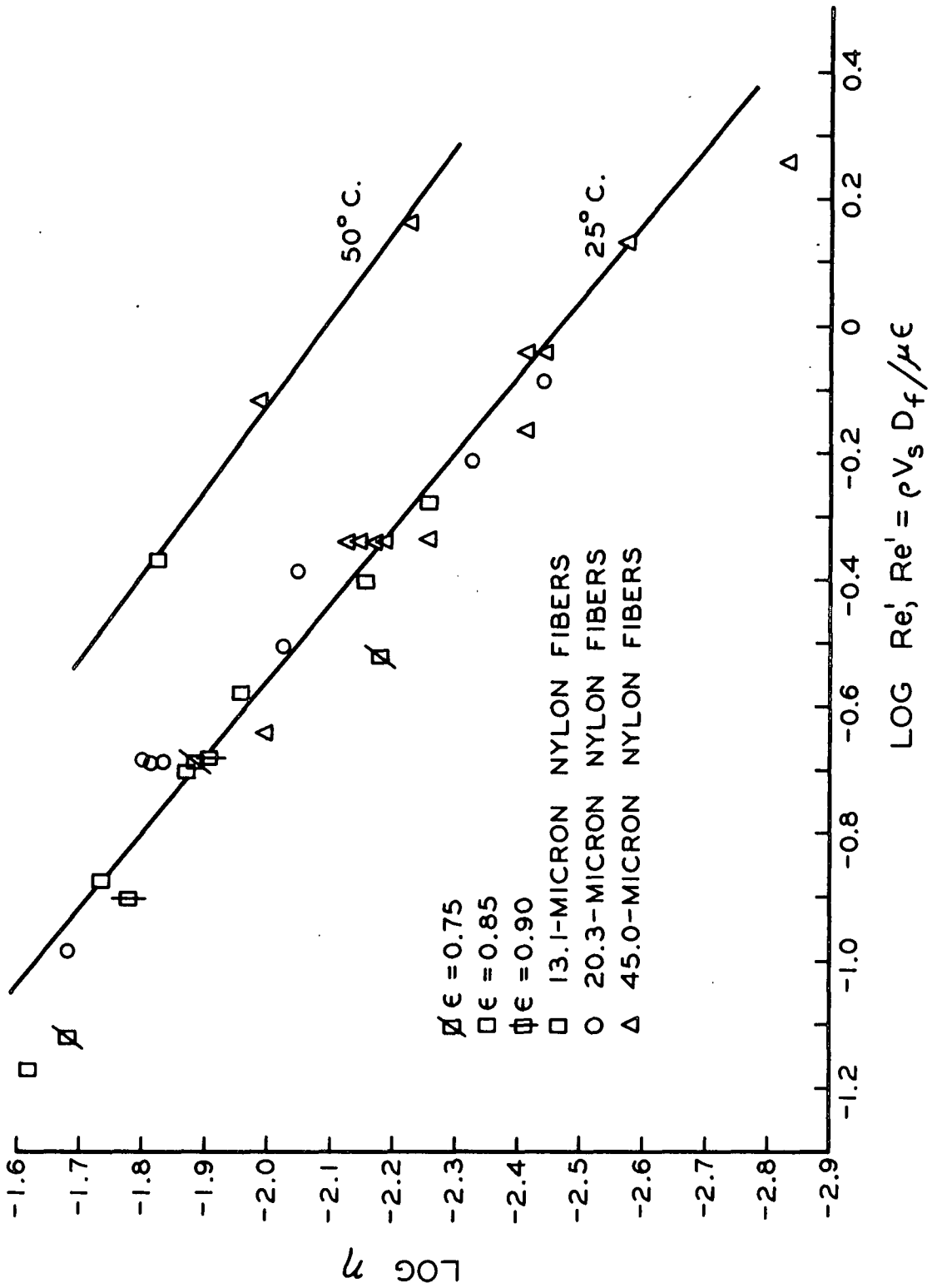


Figure 22. Final Correlation of Data

Equation (17) and Dorman's approach (20) [Equation (9)] suggest another test of the data to determine whether or not Brownian diffusion is the only mechanism of collection operating over the range of variables studied. According to Equation (17), if the data were plotted as  $\eta$  versus  $(\text{Re}')^{-0.83}$ , it should fall about two straight lines passing through the origin if Brownian diffusion is the only mechanism of collection operating. If flow-line interception were a significant mechanism of collection, the value of  $\eta$  at  $(\text{Re}')^{-0.83}$  equal to zero should be greater than zero. If inertial impaction were a significant mechanism of collection, the lines through the data points should curve upward at low values of  $(\text{Re}')^{-0.83}$  instead of being straight. The data are plotted in Fig. 23, and with the exception of one data point, the data fall about two straight lines that pass through the origin. The data also show no tendency to curve upward at low values of  $(\text{Re}')^{-0.83}$ . Therefore, flow-line interception and inertial impaction were not significant mechanisms of collection.

From Equation (17), it can be seen that the ratio of the slopes of the two lines passing through the data points in Fig. 23 must be equal to the ratio of the two Schmidt numbers raised to the power  $\underline{c}$ . The value of  $\underline{c}$  calculated in this manner is -0.77.

#### PHYSICAL SIGNIFICANCE OF THE CORRELATION

At a constant Reynolds number, the flow pattern is exactly the same around cylindrical fibers of different diameters. Also, the time for a fluid element in a streamline to pass a given fiber is proportional to  $1/\underline{V_s}$ . Therefore, the time in which diffusion can take place is proportional

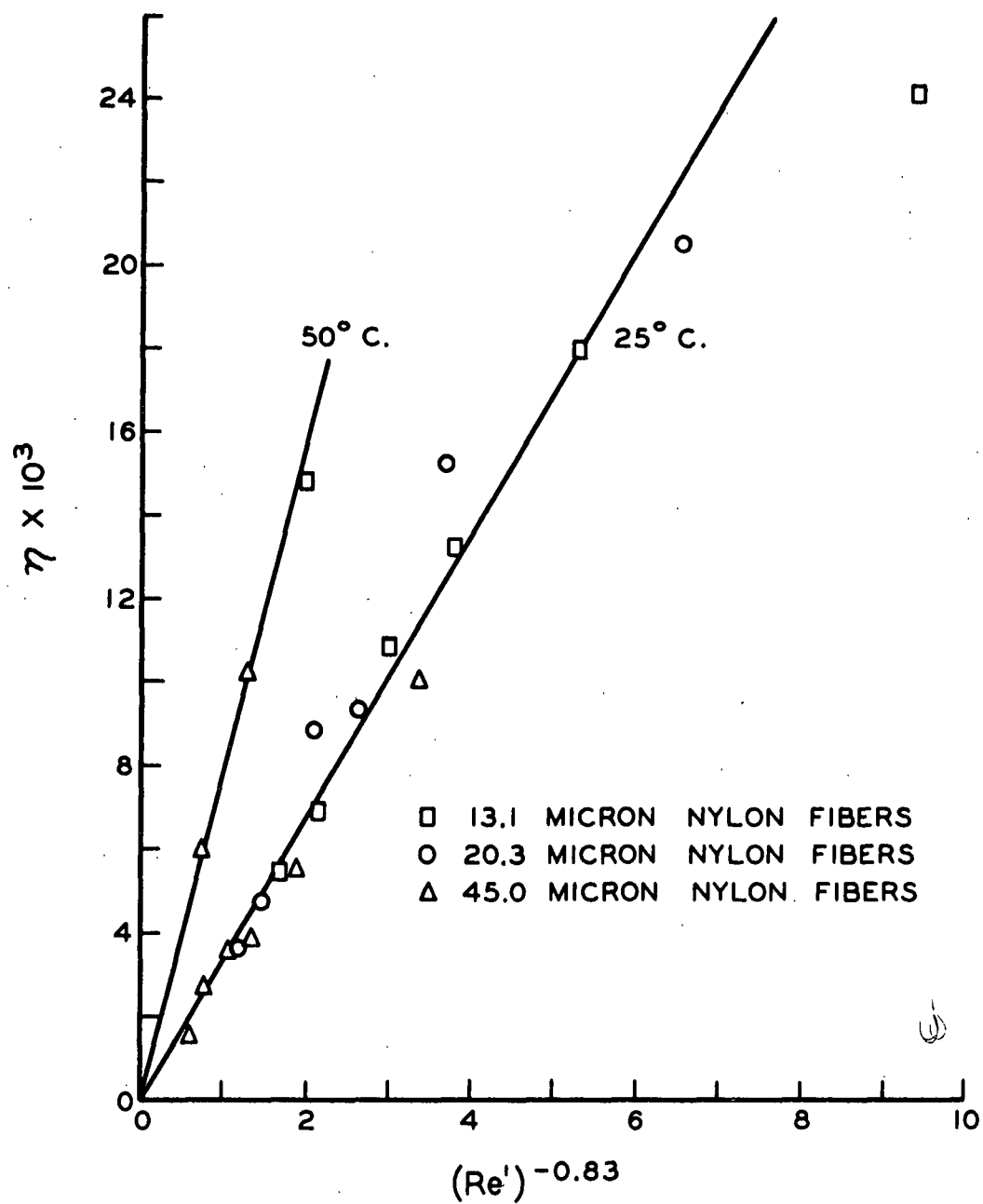


Figure 23. Plot of  $\eta$  versus  $(Re')^{-0.83}$

to  $1/\underline{V}_s$ , and from this standpoint,  $\eta$  should be proportional to  $1/\underline{Re}'$ . However, at increasing Reynolds number, the streamlines come closer to the fiber, and the distance the particles have to move by diffusion is decreasing. Therefore, the exponent on the Reynolds number should be somewhere between -1 and 0.

#### COMPARISON OF DATA WITH THEORETICAL RESULTS

As stated previously, Langmuir (11) and Friedlander (24) have derived equations predicting the effective fiber efficiency for a single cylinder in an infinite medium. These can be simplified (23) to the following:

$$\eta_o = 0.335 \pi / (2 - \ln Re)^{0.4} (Re)^{0.6} (Sc)^{0.6} \quad (18)$$

(Langmuir)

$$\eta_o = 0.568 \pi / (2 - \ln Re)^{1/3} (Re)^{2/3} (Sc)^{2/3} \quad (19)$$

(Friedlander)

The above equations have nearly the same form as Equation (17), which fits the data of this study (the influence of the term,  $[2 - \ln Re]^{-1/3}$ , is small compared to  $Re^{-2/3}$ , though in the opposite direction). However, for values of  $\underline{Re} = 0.1$  and  $\underline{Sc} = 1.76 \times 10^6$ , Equations (18) and (19) predict values of  $\eta_o$  of  $4.2 \times 10^{-4}$  and  $3.4 \times 10^{-4}$ , respectively, while the experimental value of  $\eta$  was  $2.3 \times 10^{-2}$ . The experimental value of  $\eta$  is over 50 times larger than the theoretically predicted values. This discrepancy can be partially explained by the following two reasons:

1. Equations (18) and (19) were derived for a single cylinder in an infinite medium. When the cylindrical fibers are in a mat of fibers, the interfiber interference causes the streamlines to curve more around the

fibers. This increased curvature of the streamlines brings the particles closer to the fiber, and they stay closer to the fiber for a longer period of time, increasing the retention by diffusion.

2. Equations (18) and (19) were derived for a smooth cylinder, i.e., to predict the initial retention. From Fig. 16, it can be seen that the initial retention is much lower than the average. For that particular run, one can roughly calculate from the curve in Fig. 16 that the initial value of  $\eta$  is a factor of 8 lower than the average value.

The exponents on the Reynolds number and the Schmidt number in Equation (17) are appreciably higher than the exponents in Langmuir's and Friedlander's theoretical equations [Equations (18) and (19)]. This may be due to the fact that the instantaneous value of the effective fiber efficiency is a function of the amount of titanium dioxide already present in the mat. Therefore, the average value of the effective fiber efficiency,  $\eta$ , is a function of the total amount of titanium dioxide retained.

Now, if one were to compare the instantaneous effective fiber efficiency at the end of two experimental filtrations, the first at a high Reynolds number and the second at a low Reynolds number, it would be found to be lowest in the first case. The instantaneous effective fiber efficiency would be lower in the first case, partially due to the change in the flow pattern around the fibers [which is accounted for in Equations (18) and (19)], and also partially due to the fact that the total amount of titanium dioxide retained in the mat is lower. Therefore, the variation in the average effective fiber efficiency caused by a change in the Reynolds

number should be greater than that predicted theoretically. (The experimentally determined exponents on the Reynolds number and Schmidt number were -0.8, as compared with -0.6 and -0.67.)

## SUMMARY AND CONCLUSIONS

### APPROACH USED

A study was made of three of the factors which influence the removal of titanium dioxide particles from a water suspension by the internal structure of a filter mat comprised of cylindrical nylon fibers randomly oriented in the plane perpendicular to the direction of flow: fluid velocity, fiber diameter, and mat porosity.

When the flow pattern around an infinite cylinder in an infinite fluid and the relative motion of a particle in a fluid were considered, four possible mechanisms of collection of a particle by a cylinder were apparent: (1) inertial impaction, (2) flow-line interception, (3) Brownian diffusion, and (4) settling.

The experimental procedure consisted of passing a dilute suspension of titanium dioxide particles through a mat of nylon fibers at constant velocity, and analyzing the mat to determine the amount of particles collected. The filter mats were preformed and compacted with a permeable piston to obtain a uniform porosity. The amount of suspension used and its concentration were held constant.

### RESULTS

It was found that the instantaneous collection efficiency at constant fluid velocity, fiber diameter, and porosity was not constant, but increased from the beginning of the run to the end. This meant that the collection efficiency data obtained in a given experimental run was



an average value which was a function of the total amount of titanium dioxide passed to the filter mat.

The filter mat was considered to be a network of cylindrical fibers, all having the same effective fiber collection efficiency,  $\eta$ . A differential material balance across one fiber layer was integrated over the entire mat thickness to yield the following equation:

$$\ln[W_o/(W_o - W_{mat})] = 4\alpha h \eta/\pi D_f \quad (14)$$

Experiments in which the filter mats were sectioned and the sections analyzed showed that Equation (14) fit the data, and that  $\eta$  was constant over the mat thickness.

The effective fiber collection efficiency,  $\eta$ , in Equation (14) was found to be equal to:

$$\eta = 2.3 \times 10^{-3} (Re')^{-0.8} (Sc)^{-0.8} \quad (17)$$

where:

$$Re' = \rho \underline{V_s} \underline{D_f} / \mu \epsilon$$

$$Sc = \mu / \rho \underline{D_{BM}}$$

$$\underline{D_{BM}} = \underline{kT} / 3\pi \mu \underline{D_p}$$

This correlation fits the data over the following ranges of the variables studied:

$\underline{D_f}$ , fiber diameter, 13.1 to 45.0 microns

$\epsilon$ , mat porosity, 0.75 to 0.90

$\underline{V_s}$ , superficial fluid velocity, 0.39 to 3.09 cm./sec.

The titanium dioxide particles used had an average diameter of 0.96 micron. The temperature of the system was changed from 25 to 50°C. to determine the influence of the Schmidt number.

### CONCLUSIONS

The cylindrical fiber model of a fibrous filter mat has been shown to be very useful in interpreting studies of retention of fine particles by the internal structure of the mat.

It has been shown that the average value of the effective fiber collection efficiency,  $\eta$ , for a given experimental run was constant from the upstream side of the filter mat to the downstream side. However, the instantaneous value of  $\eta$  in an experimental filtration run was not constant, but was very dependent on the amount of particles that had already been retained by the fibers. This was apparently due to the particle deposits changing the surface of the fibers, which in turn changed the flow pattern around the fibers.

The average value of the effective fiber collection efficiency was very dependent on the ionic conditions of the system. This was due to preferential adsorption of ions at the surfaces of the fibers and the particles. Under certain conditions (i.e., high pH and low total ionic concentration, such as occurred when the fibers and particles were dispersed in Appleton city water), the adsorbed ions resulted in a charge high enough so that the fibers and particles repelled each other and the effective fiber collection efficiency was essentially zero.

Brownian diffusion was apparently the only significant mechanism by which the titanium dioxide particles moved across the streamlines toward the nylon fibers over the range of variables investigated in this study. While it seems improbable that settling was a significant mechanism of collection in this study, the available data do not permit the elimination of this possibility.

#### FUTURE WORK

While this study has shown that the cylindrical fiber theory of retention, which was originally applied to fibrous air filter mats, is also applicable to fibrous mats used in solution clarification, many questions in this field remain unanswered. Some of these questions are:

1. The effect of fiber shape and surface roughness
2. The effect of the surface energies of the fibers and the particles
3. The effect of higher velocities
4. The effect of larger particle sizes.

The answers to these questions will not only aid in the design of solution clarification equipment, but they are essential to the eventual understanding of the phenomenon of retention of inorganic fillers and cellulosic fines in the formation of a sheet of paper.

This study has been carried out with smooth, cylindrical nylon fibers. As the deposits of titanium dioxide particles formed, the shape and surface roughness of the fibers was changed. This coincided with an increase in the amount of titanium dioxide retained by the mat,

and an increase in the pressure drop across the mat. Both of these changes were large, indicating that the shape and surface roughness of the fibers in the mat are important variables which should be studied. These two variables might be studied using rayon fibers. Cuprammonium rayon fibers are smooth and almost cylindrical, while viscose fibers have a very irregular cross section, usually a scalloped margin. Also, the degree of irregularity and surface roughness of viscose fibers can be controlled to a certain extent (25).

Regardless of the mechanism by which a particle in an aqueous suspension and a fiber in a filter mat are brought into contact, or close proximity, the main forces which will cause the particle to be retained by the fiber are Van der Waal's forces. These forces of attraction must be stronger than any combination of forces acting to remove the particle (fluid drag forces, repulsive forces due to adsorbed ions, and the kinetic energy of the particle). Therefore, in future work the surface energies of the particles and fibers should be considered. It is possible that not only are ions adsorbed at the solid-liquid interface, but molecules as well. If this is the case, then it might be possible for particles in a suspension containing small amounts of a soap or detergent to adsorb a monomolecular layer of these molecules with the polar group at the solid surface and the nonpolar group at the liquid surface. This would result in a lower energy surface, which could reduce the retention.

The experiments in solution clarification to date have been carried out at low fluid velocities, considering that the maximum

fluid velocity in some papermaking systems may be over one hundred centimeters per second. In air filtration, inertial impaction becomes an important mechanism of retention at high velocities. Wong's (10) experiments showed that inertial impaction became a significant mechanism at values of  $\psi$  over 0.6. If a value of  $\psi$  equal to 0.6 is used as a criterion, inertial impaction cannot become a significant mechanism for the removal of one-micron titanium dioxide particles from a water suspension by a mat of 13.1-micron fibers at superficial velocities under  $3.6 \times 10^3$  centimeters per second. However, collection by the inertial impaction mechanism depends not only on  $\psi$ , but also on the Reynolds number. At a constant value of  $\psi$ , the Reynolds number for the aqueous system is about 100 times greater than for air. This means that the streamlines will curve much more sharply as they approach the fiber, and will come much closer to the fiber, both factors increasing the probability of retention by the inertial impaction mechanism. Any attempt to predict the conditions under which inertial impaction will be an important mechanism of retention is further complicated by the fact that the fluid drag force tending to remove the particles from the fibers is greater in a liquid system than in air, even at constant Reynolds number.

The question of whether inertial impaction will become an important mechanism at velocities of interest in papermaking systems, or whether the fluid drag forces at these velocities are too great to permit retention can be answered experimentally. This could be accomplished with an apparatus similar to the one used in this study. The flow tube would have to be closed and the pump placed on the upstream side of the flow tube to obtain the high velocities. The mats used would have to be very thin to avoid excessive pressure drops and nonuniform porosities.

If inertial impaction does prove to be an important mechanism of retention, experiments with larger particles would be of interest. Collection of the particles by the inertial impaction mechanism should be a function of the square of the particle diameter. However, the fluid drag force tending to remove the particle from the fiber should also be a strong function of the particle size.

When larger particles are used, settling may become a significant mechanism of collection. This could be demonstrated by reversing the direction of flow through the mat from vertically down to vertically up. A significant decrease in the amount of particles retained would indicate that settling is a significant mechanism of collection. If the amount of particles retained decreased drastically, it would indicate that settling was the controlling mechanism of collection.

The effect of ionic conditions on retention should be investigated further, especially with respect to papermaking systems. Alum is usually added to papermaking systems for pH control. It would be of interest to know whether the aluminum ion concentration is high enough to eliminate repulsion effects due to adsorbed ions. It would also be of interest to know if the filler materials in the papermaking suspension are present as free particles, or if they are trapped in a gelatinous aluminum hydroxide precipitate which is then retained by the fibers.

# NOMENCLATURE

<u>A</u>	= face area of mat, sq. cm.
<u>a</u>	= a constant
<u>B</u>	= a constant
<u>b</u>	= a constant
<u>c</u>	= a constant
<u>d</u>	= differential operator
<u>D</u>	= the diffusion parameter
<u>D<sub>BM</sub></u>	= the effective diffusion coefficient of a particle, sq. cm./sec.
<u>D<sub>f</sub></u>	= diameter of a fiber, cm.
<u>D<sub>p</sub></u>	= diameter of a particle, cm.
<u>E</u>	= Dorman's diffusion parameter
<u>e</u>	= 2.718, base of natural logarithms
<u>G</u>	= settling parameter, $\frac{V_g}{V_s}$
<u>g</u>	= acceleration due to gravity, 981 cm./sec. <sup>2</sup>
<u>h</u>	= mat thickness, cm.
<u>I</u>	= Dorman's inertial impaction parameter
<u>k</u>	= Boltzman's constant, $1.380 \times 10^{-16}$ erg/deg.
log	= common logarithm
ln	= natural logarithm
<u>L</u>	= length of fibers per unit volume of mat, cm.
<u>N</u>	= number of particles per unit volume of fluid, cm. <sup>-3</sup>
<u>N<sub>h</sub></u>	= number of particles per unit volume of fluid at a mat thickness <u>h</u> , cm. <sup>-3</sup>
<u>N<sub>o</sub></u>	= number of particles per unit volume of fluid entering the mat, cm. <sup>-3</sup>
<u>R</u>	= the flow line interception parameter, $\frac{D_p}{D_f}$

- $\underline{Re}$  = Reynolds number based on a cylinder,  $\rho \frac{\underline{V}_s \underline{D}_f}{\mu}$
- $\underline{Re}'$  = modified Reynolds number based on a fiber in a mat,  
 $\rho \frac{\underline{V}_s \underline{D}_f}{\mu} \epsilon$
- $\underline{Sc}$  = Schmidt number,  $\mu/\rho \underline{\ell} \frac{\underline{D}_{BM}}{\underline{\ell}}$
- $\underline{t}$  = time, sec.
- $\underline{T}$  = absolute temperature, degrees Kelvin
- $\underline{V}_g$  = free settling velocity of a particle, cm./sec.
- $\underline{V}_o$  = velocity of an infinite fluid stream, cm./sec.
- $\underline{V}_s$  = superficial velocity, cm./sec.
- $\underline{W}$  = cumulative mat weight, grams
- $\underline{W}_o$  = weight of particles fed to the mat, grams
- $\underline{W}_h$  = weight of particles passing through the mat at the mat  
thickness of  $\underline{h}$ , grams
- $\underline{W}_{mat}$  = weight of particles collected by the mat, grams
- $\underline{x}$  = average displacement of a particle in a time,  $\underline{t}$ , cm.
- $\underline{x}_o$  = effective thickness of the fluid layer from which particles  
are removed by diffusion and direct interception, cm.
- $\alpha$  = mat solid fraction
- $\gamma$  = Dorman's attenuation factor
- $\epsilon$  = porosity,  $1 - \alpha$
- $\eta_o$  = effective fiber collection efficiency of a single cylinder  
in an infinite medium
- $\eta$  = effective fiber collection efficiency of a single fiber in  
a mat of fibers
- $\rho \underline{\ell}$  = fluid density, g./cc.
- $\rho \underline{p}$  = particle density, g./cc.
- $\psi$  = inertial impaction parameter,  $(\rho \underline{p} - \rho \underline{\ell}) \underline{V}_o \underline{D}_p^2 / 18 \mu \underline{D}_f$
- $\mu$  = fluid viscosity, poises



#### ACKNOWLEDGMENTS

The author would like to express his appreciation to Dr. William Ingmanson and the other members of the thesis advisory committee for the advice and encouragement they have given throughout this investigation.

The assistance of Leonard Dearth and Keith Hardacker in the design of the light-scattering apparatus is also appreciated.

LITERATURE CITED

1. Scheidegger, Adrian E. The physics of flow through porous media. New York, The Macmillan Company, 1957. 236 p.
2. Whitney, R. P., Ingmanson, W. L., and Han, S. T. Some aspects of permeation, filtration, and fluidization. Tappi 38, no. 3:157-66 (March, 1955).
3. Ingmanson, W. L., Andrews, B. D., and Johnson, R. C. Tappi 42, no. 10:840-9(Oct., 1959).
4. Hermans, P. H., and Brédee, H. L., J. Soc. Chem. Ind. 55T:1-4T (Jan. 10, 1936).
5. Grace, H. P., A.I.Ch.E. Journal 2, no. 3:317-36(Sept., 1956).
6. Dawkins, George S. Electrostatic effects in the deposition of aerosols on cylindrical shapes. Doctor's Dissertation. Urbana, Ill., The University of Illinois, 1957. 68 p. University Microfilms No. 23316.
7. Holtzman, William. The application of the Verwey and Overbeek theory to the stability of kaolinite-water systems. Doctor's Dissertation. Appleton, Wisconsin, The Institute of Paper Chemistry, 1959. 160 p.
8. Friedlander, S. K., and Johnstone, H. F., Ind. Eng. Chem. 49, no. 7:1151-6(July, 1957).
9. Saxton, R. L., and Ranz, W. E., J. Appl. Phys. 23, no. 8:917-23 (Aug., 1952).
- X 10. Wong, J. B., Ranz, W. E., and Johnstone, H. F., J. Appl. Phys. 27, no. 2:161-9(Feb., 1956).
- X 11. Langmuir, I., OSRD-865, as quoted by Chen, C. Y. (26).
12. Lamb, Horace. Hydrodynamics. 6th ed. England, Cambridge University Press, 1932.
13. Ranz, W. E. The impaction of aerosol particles on cylindrical and spherical collectors. Atomic Energy Commission unclassified document SO-1004. Univ. of Illinois, March 31, 1951.
14. Grace, H. P. The art and science of liquid filtration. In Reaction kinetics and unit operations. Chem. Eng. Progr. Symposium Ser. 25, no. 25:151-61(1959).
15. Thomas, J. W., and Yoder, R. E., A.M.A. Arch. Ind. Health 13:550-5 (June, 1956).

16. Rahm, Joseph A., Determination of titanium in pigments and ores. Anal. Chem. 24, no. 11:1832-3(Nov., 1952).
17. Thomas, David Glen. Deposition of aerosol particles in fibrous packing. Doctor's Dissertation. Columbus, Ohio, Ohio State University, 1953. 246 p.
18. Marshall, Charles G. Deposition of aerosol particles on screens. Doctor's Dissertation. Columbus, Ohio, Ohio State University, 1956. 264 p. University Microfilms, No. 17,392.
19. Humphrey, Arthur E. Air sterilization by fibrous media. Doctor's Dissertation. New York, Columbia University, 1953. 121 p. University Microfilms, No. 15,632.
20. Dorman, R. G. The role of diffusion, interception and inertia in the filtration of airborne particles. In Richardson's Aerodynamic capture of particles. p. 112-22. New York, Pergamon Press, 1960.
21. Haslam, J. H., and Steele, F. A. The retention of pigments in paper. Paper Trade J. 102, no. 2:36-9(Jan. 9, 1936).
22. Glasstone, Samuel. Textbook of physical chemistry. 2d ed. p. 261. New York, D. Van Nostrand Company, Inc., 1946.
23. Dobry, R., and Finn, R. K. Mass transfer to a cylinder at low Reynolds numbers. Ind. Eng. Chem. 48, no. 9:1540-3(Sept., 1956).
- ✓ 24. Friedlander, S. K., A.I.Ch.E. Journal 3, no. 1:43-8(March, 1957).
25. Ott, Emil, and Spurlin, Harold M., ed. Cellulose and cellulose derivatives. 2d ed. p. 379-92. New York, Interscience Publishers, Inc. 1954.
26. Chen, C. Y., Chem. Revs. 55, no. 3:595(June, 1955).
27. Ghosh, G., Water and Water Eng. 62:145-73(1958).
28. Eliassen, Rolf, J. Am. Water Works Assoc. 33, no. 5:926-42(May, 1941).
29. Mossman, C. E., and Mason, S. G., Can. J. Chem. 37, no. 7:1153-64 (July, 1959).
30. Harris, Milton, and Sookne, Arnold M., J. Research Natl. Bur. Standards 26:289-92(April, 1941).

## APPENDIX I

### EFFECT OF IONIC CONDITIONS ON RETENTION

#### FORMATION OF A STABLE TITANIUM DIOXIDE SUSPENSION

Titanium dioxide was chosen as the most suitable particle because of the comparative ease of preparing stable suspensions having a narrow size range.

The preparation of stable titanium dioxide suspensions depends on the ability of the surfaces of the particles to adsorb preferentially certain ionic species and obtain a surface charge. If the surface charge is high enough and the ionic concentration of the suspension is low enough, the electrostatic forces of repulsion between the particles will be higher than the Van der Waal's forces of attraction.

However, nylon fibers will also preferentially adsorb ions, producing a surface charge. If the ionic conditions are such that the same ions are adsorbed on the fibers as on the particles, there will be a repulsive force between the particles and the fibers.

#### EXPERIMENTS LEADING TO THE SELECTION OF THE PRESENT SUSPENSION MEDIA

The first experiments were carried out with filtered and softened Appleton city water, a small aliquot of the stable titanium dioxide suspension being added to the water to form the final suspension. The pH of the city water and the final suspension was about 9.6, and the retention was almost zero. The high pH and low retention suggested the possibility that both the fibers and the particles carried a negative charge due to adsorbed hydroxyl ions, causing them to repel each other.

A series of experiments was made in which sulfuric acid was added to the final suspension to reduce the pH. The retention was approximately constant from pH 9.7 to 5. However, as the pH was reduced from 5 to 2,  $\eta$  increased by a factor of about a hundred. This substantiated the adsorbed hydroxyl ion theory, and suggested that the diffuse double layer phenomenon was very important and had to be eliminated before the study could proceed along the lines originally proposed.

There are two ways in which the repulsive forces due to the diffuse double layer can be reduced: The concentration of the ionic species that is being preferentially adsorbed can be reduced; and the total ionic concentration can be increased to reduce the thickness of the double layer. If the ionic concentration is high enough, the thickness of the diffuse double layer can be reduced to the point where the Van der Waal's attractive forces are always larger than the repulsive forces.

The next step was an attempt to reduce the thickness of the diffuse double layer by increasing the ionic concentration. A series of experiments were made in which the pH of the final suspension was adjusted to 3.0, and varying amounts of sodium chloride were added. The effective fiber efficiency,  $\eta$ , increased rapidly as the sodium chloride concentration was increased to about  $5 \times 10^{-2}$  molar, and continued to increase slowly as the concentration was increased to about  $2 \times 10^{-1}$  molar. The total increase in  $\eta$  was a factor of ten. The results of these experiments showed that the repulsive effects of adsorbed ions could be minimized, but that it required large amounts of sodium chloride (up to five pounds per run). Application of the Schulze-Hardy rule indicated that the ionic

concentration required could be drastically reduced by the use of a salt having a divalent or trivalent cation.

A series of experiments were made using aluminum chloride to increase the ionic concentration. This worked very well at concentrations below  $4 \times 10^{-4}$  molar, but occasionally a precipitate was observed in the suspension. The use of aluminum ion was discontinued in favor of calcium chloride to avoid the possible criticism that a gelatinous, invisible precipitate of aluminum hydroxide had been a collector for the titanium dioxide.

A series of experiments using calcium chloride to increase the ionic concentration showed that  $\eta$  increased rapidly with increasing calcium chloride concentration up to a concentration of  $9 \times 10^{-3}$  molar; above this concentration,  $\eta$  was apparently constant. A series of four experiments was then made under exactly the same conditions to check the reproducibility of the measurements. The variation in  $\eta$  was over 80%. However, it was noticed that the results of two of the runs which were made on the same day agreed within 10%. This indicated that the ionic character of the city water was changing from day to day, and it was decided to use deionized water instead of city water.

The first experiments with deionized water were made using the same ionic conditions used in the latest experiments with city water, but the value of  $\eta$  obtained was a factor of ten lower. This indicated that some material beneficial to retention had been removed on deionization, or that some material that reduced retention had been added.

Some preliminary experiments with deionized water, using hydrochloric acid to adjust the pH to 4, indicated that  $\eta$  was constant at calcium chloride concentrations above  $2 \times 10^{-2}$  molar. However, two further experiments, made several days apart, showed a 50% increase in  $\eta$  as the calcium chloride concentration was decreased from 5 to  $2 \times 10^{-2}$  molar. A check of the deionized water system showed that, between these two runs, the cylinders containing the ion-exchange resin had been replaced. The pH of the deionized water (before adjustment) used in the first experiment was 4.5, while that used in the second was 9.5. These results showed that the composition of the deionized water was not constant, and that the variations affected the retention results. At this point, it was decided that distilled water should be used for all retention experiments.

The first experiments using distilled water produced a value of  $\eta$  a factor of four higher than the experiments in which deionized water had been used. Several additional experiments showed that the ionic content of the water in which the fibers were deaerated and from which the mat was formed was also important. When the fibers were deaerated in city water and the mat was formed from city water,  $\eta$  was 10% lower than when the fibers were deaerated in distilled water and the mat was formed from water having the same ionic concentration as used in the retention experiment. When the fibers were deaerated in distilled water and the mat was formed from distilled water,  $\eta$  was 40% lower.

The distilled water used in this study was distilled from city water in a still set up near the equipment. The use of city water in the still resulted in rapid scale formation, even though the still pot was drained

after every 105-liter batch of water had been distilled. The experimental program was about half completed when a new source of deionized water was piped to within a few feet of the still. It was decided to feed deionized water to the still to eliminate the problem of scale formation. However, the use of water distilled from deionized water rather than water distilled from city water resulted in a decrease in  $\eta$  by a factor of about four, so it was discontinued.



## APPENDIX II

TABLE II

Run Number	$\frac{D}{f}$ , microns	$\epsilon$	DATA			
			$\frac{V}{s}$ , cm./sec.	$\frac{Re'}{f-s} = \frac{\rho D \frac{V}{f-s}}{\mu \epsilon}$	$\eta \times 10^3$	$\frac{W}{s_{mat}}$ , grams
105	13.1	0.850	0.39	0.067	24.2	0.999
98	13.1	0.850	0.78	0.134	18.1	0.908
104	13.1	0.849	1.17	0.201	13.3	0.785
103	13.1	0.850	1.55	0.266	10.9	0.694
121	13.1	0.850	2.32	0.398	6.88	0.508
122	13.1	0.850	3.09	0.531	5.50	0.439
126	13.1	0.748	0.39	0.076	20.9	0.958
127	13.1	0.751	1.55	0.301	6.65	0.504
128	13.1	0.900	0.78	0.127	16.6	0.874
91	20.3	0.850	0.39	0.104	20.6	0.793
92	20.3	0.850	0.78	0.207	15.3	0.662
84	20.3	0.850	0.78	0.207	15.6	0.679
99	20.3	0.849	0.78	0.207	14.6	0.640
90	20.3	0.850	1.17	0.312	9.43	0.476
89	20.3	0.850	1.55	0.412	8.85	0.458
119	20.3	0.849	2.32	0.617	4.68	0.269
120	20.3	0.850	3.09	0.822	3.64	0.216
93	20.3	0.899	0.83	0.208	12.3	0.580
94	20.3	0.800	0.73	0.207	15.7	0.687
95	20.3	0.750	0.69	0.207	13.0	0.600
102	45.0	0.851	0.39	0.230	10.1	0.262
96	45.0	0.849	0.78	0.461	5.53	0.153
115	45.0	0.850	0.78	0.460	6.70	0.185
131	45.0	0.849	0.78	0.461	7.07	0.192
130	45.0	0.850	0.78	0.460	7.35	0.199
134	45.0	0.850	0.78	0.460	6.50	0.178
101	45.0	0.850	1.17	0.692	3.83	0.107
100	45.0	0.849	1.55	0.913	3.57	0.101
116	45.0	0.849	1.55	0.913	3.79	0.108
117	45.0	0.850	2.32	1.367	2.66	0.075
118	45.0	0.850	3.09	1.824	1.46	0.043
123 <sup>a</sup>	45.0	0.850	0.78	0.742	10.2	0.266
124	45.0	0.850	1.55	1.460	5.95	0.164
125	13.1	0.850	1.55	0.429	14.8	0.826

<sup>a</sup> Runs 123, 124, and 125 were made at 50°C. All others were made at 25°C.